Evidence

Validation of landfill methane measurements from an unmanned aerial system

Project SC160006

We are the Environment Agency. We protect and improve the environment.

Acting to reduce the impacts of a changing climate on people and wildlife is at the heart of everything we do.

We reduce the risks to people, properties and businesses from flooding and coastal erosion.

We protect and improve the quality of water, making sure there is enough for people, businesses, agriculture and the environment. Our work helps to ensure people can enjoy the water environment through angling and navigation.

We look after land quality, promote sustainable land management and help protect and enhance wildlife habitats. And we work closely with businesses to help them comply with environmental regulations.

We can't do this alone. We work with government, local councils, businesses, civil society groups and communities to make our environment a better place for people and wildlife.

Author(s):
Dr Grant Allen[1]
Dr Paul Williams[1]
Dr. Hugo Ricketts[1]
Mr. Adil Shah [1]
Dr Peter Hollingsworth[2]
Mr Khristopher Kabbabe[2]
Mr. Jonathan Helmore [3]
Mr. Andrew Finlayson [3]
Mr. Rod Robinson [3]
Dr Tristan Rees-White[4]
Dr Richard Beaven[4]
Dr Charlotte Scheutz[5]
Dr Anders Fredenslund[5]

1 Centre for Atmospheric Science, University of Manchester
2 School of Mechanical, Aerospace and Civil Engineering, University of Manchester
3 Emissions and Atmospheric Metrology Group, National Physical Laboratory
4 Faculty of Engineering & The Environment, University of Southampton
5 Department of Environmental Engineering, Technical University of Denmark

Evidence at the Environment Agency

Scientific research and analysis underpins everything the Environment Agency does. It helps us to understand and manage the environment effectively. Our own experts work with leading scientific organisations, universities and other parts of the Defra group to bring the best knowledge to bear on the environmental problems that we face now and in the future. Our scientific work is published as summaries and reports, freely available to all.

This report is the result of research commissioned by the Environment Agency's Research, Analysis and Evaluation group.

You can find out more about our current science programmes at
https://www.gov.uk/government/organisations/environment-agency/about/research

If you have any comments or questions about this report or the Environment Agency's other scientific work, please contact reserach@environment-agency.gov.uk.

Professor Doug Wilson
Director, Research, Analysis and Evaluation

Executive summary

Methane is an important greenhouse gas and emission controls for methane are a part of the international Paris Agreement and UK national strategies to reduce greenhouse gas emissions.

Landfill gas is mainly composed of methane and carbon dioxide, in near equal measure. While modern UK landfills capture and use much of the methane gas produced, some methane is emitted to the atmosphere. However, the precise amount of methane arising from UK landfills remains highly uncertain. The work described in this report represents a new method for precisely quantifying landfill methane emissions that has the potential to be widely used.

A feasibility study commissioned by the Environment Agency in 2013 identified that the use of unmanned aerial systems (UAS) to quantify methane emissions from landfills was a viable new measurement approach. A field trial at a UK landfill in 2015 demonstrated that it was possible to derive an emission flux of methane with a known uncertainty using in situ UAS-mounted instrumentation.

This report presents the results of a subsequent validation field trial of the UAS technology and flux-calculation approach. The aim of the field trial was to release controlled fluxes of methane gas in order to test how well the UAS approach evaluated the controlled flux.

Methane fluxes were emitted at a rate below that typically expected of UK landfills: the maximum emission rate of methane was just over 10 kg/h. This emission rate allowed the system to be tested and validated at the lowest limit of sensitivity needed for UK landfills and allowed for the characterisation of flux uncertainty to be improved in order to inform future operational use of the method.

The validation field trial took place at the UK Meteorological Office site in Cardington, Bedfordshire, UK, between 31 October and 4 November 2016.

A total of seven UAS flights were analysed. These sampled methane concentrations from a UAS downwind of the controlled emission source. The calculations of the methane fluxes were conducted without knowing the emission rate of the controlled source.

The UAS validation experiments successfully characterised the methane releases. The measured methane flux, taking into account the measurement uncertainty, always overlapped with the controlled methane emission rate. For the 7 flights, the mean percentage difference between the measured and emitted methane flux was an overestimate of 6% with a mean absolute difference an overestimate of 0.4 kg/h.

Other experiments undertaken as part of the field trial have demonstrated that the method can also detect very small methane fluxes (down to 0.15 kg/h) with comparable relative uncertainties to those calculated for flux rates over an order of magnitude higher. These small flux rates are similar in magnitude to the small point source emissions that may be expected from fugitive emissions in natural gas infrastructure. The method developed here may therefore have significant utility in the monitoring and measurement of fugitive methane emission flux rates from other UK industrial infrastructure.

The following conclusions have been reached regarding the expected performance of the method:

- The flux derived using mass balancing can be considered to be accurate to within one standard deviation, when all sources of variability and error are known or measured

- Repeated flights (or increased sampling time) can significantly reduce the uncertainty in the measured methane flux

- Sampling when the wind speeds, wind directions, and background concentrations are constant would lead to reduced uncertainty

- Further improvements to the accuracy of flux calculation could be made by appropriate measurement of wind speed and direction on board the UAS platform

- A nearby wind measurement on an elevated tower (preferably at 10 m above local ground level) remains a good substitute as long as the tower is placed in an environment representative of the intended UAS sampling

The future use of the UAS mass balance approach should always consider the following:

- Appropriate zoning of downwind areas to ensure that the sampling captures the landfill plume

- The positions of obstacles to air flow (for example any buildings) and site topography between the site and measurement location should be noted and considered when planning UAS sampling to optimise the sampling zone

- The locations of any other nearby methane emission sources must be noted. Ideally, these should not be upwind of the site of interest as this would affect background variability and could result in much larger systematic errors. If this is unavoidable, additional care may be needed to ensure good background measurements are recorded to better remove the extraneous source

- When establishing the regular grid pattern for sampling across the flux plane, the appropriate size of the cells in the grid should be defined by the instrument response rate and the wind speed

- The randomised sampling in the flux plane must ensure that at least 50 independent methane concentration measurements are taken within each individual grid cell

- Sampling in non-stagnant wind speeds (greater than around 2 metres per second) to reduce flux uncertainty (with the upper wind speed limit defined by the safe operating conditions of the UAS – around 10 metres per second)

In parallel with the UAS measurements, complementary measurements of the known methane releases were undertaken using a tracer gas dispersion method. This method is based on the assumption that a tracer gas released at a methane emission source will disperse in the atmosphere in the same way as the emitted methane. Assuming the air is well mixed, the methane emission rate can be calculated as a function of the ratio of the downwind measurements of the methane and tracer gas concentrations.

Using a constant release of an acetylene tracer, two separated teams undertook a total of 132 downwind plume measurement sets over five methane releases. The methane fluxes measured by the different teams were comparable and within experimental error. The tracer gas dispersion method was able to determine actual release rates to within the measurement uncertainties for all the tests other than one. For that test, the difference between the actual and measured methane rates was only 1kg/hour.

Both methane measurement techniques were successful in matching the known methane releases. The UAS and the tracer gas dispersion method have different operational constraints so together they represent options that allow methane emissions from landfills and other facilities to be quantified within a known level of uncertainty.

Contents _{_Toc492376624}

List of figures and tables

1. Introduction

1.1. Background

Methane (CH_4) gas is an important greenhouse gas in the Earth's atmosphere. Molecule for molecule it has a global warming potential equivalent to 25 times that of carbon dioxide (CO_2) over a 100 year period (IPCC 2007). While current globally-averaged molar concentrations of CH_4 are approximately only 0.5% of those for CO_2, the warming potential of CH_4 makes it an important part of any climate change mitigation strategy. To this end, national emission controls of CH_4 are a part of both the international Paris Agreement (2015) and various other UK national strategies to reduce greenhouse gas emissions.

Landfill gas is typically composed of near equal measures of CH_4 and CO_2 with trace amounts of other pollutant gases. While modern UK landfills capture and utilise much of the produced CH_4 gas, some is emitted to the atmosphere. However, the precise measurement of methane flux from UK landfill, and the integrated national inventory from this component of UK industry, remains highly uncertain. Current estimates rely on so-called bottom-up methods such as life-cycle approaches and models, which require many assumptions to be made.

The work reported here is a new monitoring and measurement method for the precise quantification of landfill CH_4 flux. While not conceived as a continuous monitoring approach, the precise measurement of three-dimensional - and especially vertical profiles of - CH_4 concentrations around landfill from unmanned aerial system (UAS) measurement platforms can yield accurate case study flux snapshots. These snapshots can be repeated to build meaningful statistics in support of more directly informed UK landfill fluxes as part of both regulatory requirements at the scale of individual landfill facilities and in the compilation of any national CH_4 inventories.

A feasibility study commissioned by the Environment Agency (Allen et al. 2014), identified that UAS present a viable new measurement approach to quantify bulk CH_4 emissions from landfills. A field trial at a UK landfill in 2015 (Allen et al. 2015) demonstrated that it was possible to derive bulk (site-integrated) net emission flux of CH_4 with a nominal and traceable uncertainty using in situ UAS-mounted instrumentation and a plume mass balancing model.

This report presents the results of a subsequent validation field trial of the UAS-platform-sensor technology and flux-calculation approach, whereby a flux measured downwind of a known CH_4 source was derived and compared in order to characterise uncertainty and statistical bias across a series of blind experiments.

1.2. This project

This project has built on experience and infrastructure developed and previously deployed successfully by a team of researchers and engineers at the University of Manchester (see Allen et al. 2014 and 2015) to test a UAS mass balance flux approach – (a model that derives CH_4 mass flux from sampled CH_4 concentrations and measured wind fields).

The aim of the project reported here was to emit controlled, yet blind (i.e. not known until after flux calculation) fluxes of CH_4 gas in order to test the ability of the mass balance approach and UAS sampling downwind to correctly evaluate the controlled flux.

Methane fluxes were emitted at a rate well below the rate typically expected of UK landfills (up to a limit imposed by the technical constraints of the release facility introduced below). This allowed the system to be tested and validated at its lowest limit of sensitivity, and (as importantly) allowed us to simultaneously improve our characterisation of flux uncertainty to best inform future operational use of the method.

This project was a close partnership between the Environment Agency and the University of Manchester School of Earth and Environmental Science, which developed and tested the flux calculation approaches, the University of Manchester School of Mechanical, Aerospace and Civil Engineering, which developed the UAS platform and sensor integration, and the National Physical

Laboratory (NPL), the UK's National Measurement Institute, which operated an established and calibrated field-deployable known release CH_4 flux simulation system.

The NPL release facility and a rotary UAS sensor platform were deployed at a UK Meteorological (Met) Office field site in Cardington, Bedfordshire, UK, between 31 October and 4 November 2016, to measure CH_4 concentrations in a three-dimensional sampling strategy. Additionally, a fixed wing UAS was deployed to measure carbon dioxide concentrations over a wider area as a complementary strategy (not reported further here as this study relates to the validation of a flux approach for CH_4)

The project consisted of five phases, described in the following sections of this report:

- Flux retrieval approach (section 2)

- Site evaluation and field campaign planning (section 3)

- Field campaign at the Met Office Cardington site (section 4)

- Data analysis, flux calculation and comparison (section 5)

- Conclusions and recommendation for implementation of the method (section 6)

The deliverables of the project were:

- A dataset of measured and emitted CH_4 gas concentrations and mass fluxes.

- This report, which describes the project, the gathered dataset and the retrieved mass balance fluxes and their comparison with known release fluxes, constrained by their corresponding accuracy and sources of uncertainty.

In parallel with the UAS measurements, the University of Southampton and the Technical University of Denmark undertook measurements of the known CH_4 releases using an entirely different approach: a tracer gas dispersion method. The method and the results of this complementary approach are discussed briefly in section 5 and described more fully in Appendix E to this report.

2. Flux retrieval approach

This section describes the methane (CH_4) flux retrieval method used in this study. The method was based on the mass balance algorithm described in Allen et al. (2015), which has been further developed and refined in response to field data and experience gathered in this project. We summarise the mass balance method here before describing the development and adaptations of the method.

2.1. The mass balance flux method

The conceptual method for determining a CH_4 flux using the principle of mass balancing requires precision measurement, and spatially geotagged sampling, of CH_4 concentration and horizontal wind velocity. A derivation of flux can then be achieved using the kriged mass balance approach of Mays et al. (2009), further described in the preceding study (see Allen et al. 2015). In the kriging approach, CH_4 mole fractions (concentrations) and wind velocities are sampled across and within a defined flux plane, which is defined by a two-dimensional surface projected perpendicular to a representative mean wind vector at a nominal distance downwind of an emission source. The concentration measurements are then interpolated onto a regularised two-dimensional grid, which must span the maximum vertical and horizontal extent of the plume morphology, using the geospatial interpolation technique known as kriging (see Myers 1991 for the mathematical formalism of kriging). Failure to map the maximal extent of the plume would result in a corresponding underestimate of mass flux. A synthetic idealised dataset was tested using the kriging method in project SC140015 (Allen et al. 2015) to illustrate the method and UAS sampling rationale.

The forward model at the heart of mass balancing is defined as the mass of CH_4 gas per unit time added to the volume of air moving through a flux plane, which is defined as:

$$F(CH_4) = \int\limits_{o}^{z} \int\limits_{A}^{B} (X_{ij} - X_0) n U_{\perp ij} dx dz$$

(Equation 1)

where:

X_{ij} is the kriged mole fraction of CH_4

X_0 is the background mole fraction of CH_4 determined by taking an average of measurements known (or assumed) to be outside of the emitted target plume.

n is the mole density of air calculated using ground-based measurements of pressure and temperature (and assumed to be constant throughout the flux plane)

$U_{\perp ij}$ is the mean wind speed component perpendicular to the flux plane, evaluated between ground level and the measured maximal height of the plume (z), and across and beyond the full width of the plume (x) between two arbitrary horizontal points, A and B.

2.2. Adapted mass balancing method for UAS sampling

In this project, we have adapted the flux-grid-interpolation method in response to UAS sampling considerations when measuring in the near-field of an emission source. In principle, the adapted method would also serve well for sampling in the far-field, though sampling time may be increased due to the need to sample a wider area (due to plume dispersion) to yield good sampling statistics. In this sense, near-field can be considered here to represent sampling downwind of a source that has not had sufficient time to mix internally over length-scales greater than that of any turbulent eddies present in the near-surface atmosphere, whereas far-field can be conceptualised as a distance downwind where plume morphology can be expected to be Gaussian in nature (as mathematically required in the idealised kriging case described in project SC140015). It is this Gaussian far-field plume morphology that is often assumed in other conventional flux-calculation methods such as Gaussian plume inversion (see Allen et al. 2014).

It is not possible to prescribe a threshold distance downwind where this transition between turbulent and Gaussian morphology can be assumed to take place without prior knowledge and modelling of the turbulent atmospheric fluid flow as a function of convective updrafts, ground obstacles and variability in the upwind wind-field. As this is not practical (or necessary), a more elegant solution to the mass balancing sampling problem has been developed here, which can be applied at any distance from a source, with accuracy improving (in principle) the closer sampling can be made to emission source. The practical accuracy of the flux calculation is then a compromise between the stated finite operational range of concentration measurement of the instrument (often referred to as dynamic range) used to measure wind and concentration (e.g. ambient concentrations must not exceed the operating range of the instrument measuring gas concentration), and the safety considerations of flying a UAS near to such sources (due to Civil Aviation Authority exclusion and site regulations).

The adapted mass balancing model and sampling rationale is as follows. Instead of kriging, a regularised grid is defined within the flux plane with a spatial spacing equal to the response time of the instrument multiplied by the measured mean wind-speed perpendicular to the flux plane. This then yields a sampling length scale that is representative of each measurement in the flux domain. For example, for a wind speed of 5 m/s and an instrument with a 0.5 Hz response time measuring CH_4 concentration, a suitable grid spacing would be 10 m x 10 m (in the horizontal/vertical plane perpendicular to wind direction). However, the choice of grid spacing must also be a compromise between the length scale that the measurement represents and the potential for including unwanted 'dead space' or areas in the flux plane that might contain very little sampling, making them unequally weighted in the final flux calculation. The implications and calculations of this for the instruments and measurements in our campaign will be described further in section 5.

All concentration measurements within the bounds of each grid cell are then averaged to obtain a single value for each grid cell within the bounds of the flux plane. An example of real UAS sampling and the resulting averaged flux grid can be seen in Figure 5.4. This method then allows for flux calculation from sampling of any turbulent (or Gaussian) plume downwind as long as the following criteria are met:

- That sampling is (ideally) equally weighted across the flux plane, which must completely encompass the maximal extent of any advected emission.

- That sampling is not significantly biased (unequally weighted) to the expected locations of the plume.

- That sampling frequency and total sampling time are sufficiently high, or long, respectively, such that the flux plane is sampled repeatedly to capture the time-varying footprint of the plume morphology on the flux plane as emissions cross it in the course of the total measurement period.

The last is perhaps the most important consideration. As a turbulent plume may be conceptualised to cross the flux plane through several (unknown and random) grid cells in the flux domain at any moment in time (the instantaneous plume footprint), and noting that this footprint may change with time, the sampling must occur as rapidly as possible, and for as long as necessary, to yield good sampling statistics of each grid cell across the entire flux plane in order to capture the mean footprint of the plume across the domain in any measurement period. In essence, the efficacy of the sampling method can be conceptualised as the correlation between the time-integrated measurement sampling density of the flux plane and the mean footprint of the advecting emission plume through it. To yield meaningful statistics, and to obtain a Gaussian uncertainty/error budget (see next section), the guidance here is that the number of concentration measurements per grid cell over the course of any measurement period should exceed 50. For example, in the illustrative case of a 0.5 Hz instrument and a grid-spacing of 10 m, this would equate to at least 100 seconds of sampling (flight time) for each grid cell in the flux plane.

2.3. Mass flux uncertainty budgeting

Equation 1 can be used as an error propagation model through which upper and lower bounds on the CH_4 flux can be calculated. This is achieved by measuring, or otherwise using knowledge about, the uncertainty implicit in each factor of the flux equation; that is, concentration measurement precision, the standard deviation of the mean concentration measurement in each grid cell in the flux plane, background (out-of-plume) concentration variability, and wind speed and wind direction variability. Each of these uncertainty terms can be expressed as a standard deviation (with Gaussian statistics). In all but the case of the measurement precision (which has its own characteristic instrumental uncertainty), this variability can be derived from measurements of wind vector and measured gas concentration. In the total flux equation, each of these errors are uncorrelated, allowing us to derive a final statistical flux uncertainty, which can be represented as the sum of error sources in quadrature for each grid cell, summed over all grid cells in the flux plane, thus:

$$\sigma_T = F \sum_i^N \sqrt{\frac{\sigma_X^2}{X} + \frac{\sigma_\varepsilon^2}{X} + \frac{\sigma_{ws}^2}{ws} + \sigma_{wd}^2 + \frac{\sigma_B^2}{B}} \quad \text{(Equation 2)}$$

where:

σ_T = Total flux uncertainty (at one standard deviation), summed over N grid cells for entire flux plane (g/s)

F = Total flux, calculated in Equation 1

σ_X = Standard deviation of measured mass concentrations in each grid cell, i (g/m^3)

σ_ε = Instrumental measurement precision (g/m^3)

X = mean measured concentration (in each grid cell, i)

σ_{ws} = Standard deviation of measured wind speed across measurement period (m/s)

ws = mean wind-speed (evaluated for entire flux plane).

σ_{wd} = Standard deviation of the cosine of wind angle variability perpendicular to flux plane (unitless)

An illustrative example of flux uncertainty by this method was described in the field trial project (Allen et al. 2015).

The flux (and flux uncertainty) method above was applied to all measurements recorded in this project and forms the basis of the results presented in section 5 and in Appendix C.

3. Site Description

This section describes the site and facilities selected for the field campaign.

As described more fully in Allen et al. (2015), UAS flight operation is subject to Civil Aviation Authority (CAA) regulations and site-specific safety considerations. These constraints broadly define a need for a controlled area (>150 m away from a congested area and 50 m away from general members of the public, buildings and property that are not under the control of the operator) for small unmanned surveillance aircraft with mass <20 kg (Air Navigation Order 2016, Art. 95). In addition to these regulatory constraints, a guiding scientific principle of this project was to select a site that was subject to minimal extraneous inputs of CH_4, such that the controlled emissions used for validation would be optimally distinct from other off-site sources such as nearby landfill or other fugitive emission. Other desirable constraints included a flat surface topography to minimize flow disturbance of controlled emissions for the purposes of an idealised conceptual validation of the mass balancing method in principle. Further desirable guiding principles included the use of a site with road access and nearby logistical facilities (storage, protection from the elements, washroom and bench provision) for human and technical needs.

The above considerations define a relatively flat field site remote from nearby potential sources of CH_4 (e.g. >1 km from any landfill or large town or city) and with a perimeter wider than at least 300 m to enable safe flight operations of the aircraft being used. The UK Met Office Cardington field site in Bedfordshire was identified as a suitable location for this work (see Figure 3.1). This site had the added advantage that airspace above it is zoned by the CAA as a permanent danger area, so the site can be safely used for development and flight testing of aircraft without endangering other airspace users. Further information on the conduct of the field campaign is given in section 4.

The Cardington site is ~600 m wide at its maximal extent (northwest to southeast) and ~400 m north to south. Office, storage and laboratory facilities were made available to the team in serviced buildings on the northern perimeter, which can be seen in Figure 3.1. Several meteorological towers (up to 50 m in height - measuring wind speed and direction and other parameters) and other ground meteorological instrumentation can be seen to the south and east of the main buildings.

Figure 3.1 - Google Earth Image of the Met Office Cardington field site

The red line defines a scale bar of 200 m. Image source: Google, DigitalGlobe.

4. Conduct of field experiments

This section describes the design and conduct of field experiments, including day-to-day field operations.

A series of varied and controlled releases of CH_4 and CO_2 gas using the NPL Controlled Release Facility (CRF - see Appendix A) was undertaken within the perimeter of the Met Office Cardington site between 1 November and 4 November 2016. A total of 16 UAS sampling flights over the course of these four days (each lasting between 16 and 28 minutes) were conducted using the tethered UAS rotary system described in Appendix B. Of these, a total of seven rotary UAS flights were conducted during controlled releases of CH_4 gas. A further two flights with a fixed-wing UAS to sample CO_2 were conducted on 3 November (described in Appendix B and Appendix D).

As a complementary and independent comparison with the results of this project, the University of Southampton and the Technical University of Denmark conducted acetylene (C_2H_2) tracer-based flux measurements (see Appendix E).

4.1. Validation Approach

The release rate (mass flux) of gas released from the CRF was varied across the campaign by the NPL team but not known to the wider project team at the time of the experiment. The flight teams were only aware of the location and elevation of emission sources at the time of processing.

This facilitated a 'blind' flux calculation exercise using the UAS measurements and the mass balance approach. The comparison between derived flux and actual flux was only made after the conclusion of the project, and only after a flux had been derived from UAS sampled data. For each flight a flux was calculated and later compared to the coincident mass flux rate reported by the NPL team.

To ensure strict compliance with this validation rationale, the various CRF mass flux rates were supplied only to the Environment Agency project manager by the NPL team after the conclusion of the field campaign. Independently calculated fluxes from the University of Manchester team were then supplied separately to the Environment Agency before being compiled for comparison in this report (see section 5 for results).

For the purposes of this validation, the following parameters are compared and reported in section 5:

- flight-by-flight CH_4 flux comparison with coincident NPL release rates to yield both absolute bias, and bias within the calculated statistical uncertainty

- mean bias (correlation) of all UAS flight flux data (compared to real flux) and aggregate standard deviation of bias (standard mean error) across all flights

This then yields a representative typical error by the mass balancing method for independent flight data and statistical error for repeated flight measurements. A further instructive parameter will be the agreement within uncertainty for each flight separately, which can yield confidence intervals on flux for any analogous future sampling.

4.2. The NPL controlled release facility and release rationale

The NPL controlled release facility (CRF) was configured to co-release near-pure CO_2 and natural gas (as CH_4 source) from up to three emission nodes (point sources separable by up to 150 m with respect to each other) positioned approximately 200 m upwind of a pre-designed UAS sampling area . A full description of the CRF and the controlled releases are provided in Appendix A.

We employed two mass fluxes between 5 kg/h and 10 kg/h for CH_4 and 10 kg/h and 25 kg/h for CO_2. The relative proportions reflect the ratio of the molar masses of the two molecules such that the concentrations in air can be configured to be equivalent. We note that flux rates for other potential point sources of interest regarding methane emissions (such as oil and gas facilities) may

typically be much lower than those we have used in this validation study. In our discussion of the results, we reflect on the transferability of this method to various emission sources in the context of the validated measurements by examining our limits of detection by the mass balancing method (section 5.4).

The focus of this project was the validation of CH_4 flux. Unfortunately, a late delivery of CH_4 gas to the field site (arriving at midday on 2 November) meant that rotary flights on 1 November sampled CO_2 releases only. Therefore, from herein, only the analysis of CH_4 flux data will be discussed, which consisted of seven flights of the rotary system on 2 and 3 November 2016. The results for an example flight with CO_2 measurements only are included in Appendix D.

At its lowest limit, the CH_4 emission rate tests and validates the method for fluxes far less than those of the lowest published scenario for known UK landfill emissions. Two release rates within the nominal range were selected by NPL for release in this experiment.

A range of experimental layouts and designs were conceived to test various sensitivities of the method to the detection of multiple, or elevated, plume release points. For example, the method needs to be robust to detect disperse and diffuse plumes from across a typical landfill site in bulk, so the use of two nodes spatially separated from each other allowed a test of the method for point sources up to 150 m apart. The effects of very near-surface turbulence and friction were also investigated by conducting releases both at the surface and slightly elevated above ground.

All release experiments occurred at either ground level or on elevated platforms at a height of approximately 6.2 m. The configuration of each CH_4 release and GPS coordinate node location on site is provided in Table 4.1 (only release configurations on days of CH_4 release are provided here).

Table 4.1 Release Data from the NPL CRF, showing date, time and location of release, and node configuration

Release number[1]	Remarks	Date and time (GMT)	Node position(s)
8	CO_2 and CH_4 release, MFC[2]#1 and MFC#2 top of tower (~6.2 m)	2/11/16 15:00 to 16:35	Co-located 52.10498N, 0.42331W
9	CO_2 and CH_4 release, MFC#1 and MFC#2 top of tower (~6.2 m)	3/11/16 10:31 to 12:19	Co-located 52.10356N, 0.42474W
10	CO_2 and CH_4 release, MFC#1 and MFC#2 from top of tower (~6.2 m)	3/11/16 14:26 to 15:29	30 m Separated nodes 52.10343N, 0.42419W
11	CO_2 and CH_4 release, MFC#1 and MFC#2 from top of tower (~6.2 m)	3/11/16 15:36 to 16:40	30 m Separated nodes 52.10343N, 0.42419W
12	CH_4 only, MFC#2, ground based release	4/11/16 08:31 to 10:00	52.10380N, 0.42391W

Note 1: Details of releases 1 to 7 (carbon dioxide only) are provided in Appendix A

Note 2: Mass Flow Control device (MFC)

4.3. UAS sampling and flight design

The University of Manchester deployed a multi-rotor UAS tethered to a 150 m Teflon sampling line that draws sampled air down to a ground-based Los Gatos Research Inc Ultraportable Greenhouse Gas Analyser (UGGA). The instrument employs infrared Off-Axis Integrated Cavity Output Spectroscopy (OA-ICOS), to measure precision CH_4 and CO_2 concentrations. For further details of the UAS and instrumentation, please see Appendix B.

Prior to each flight, a wind speed and direction measurement was recorded and a UAS sampling zone was defined downwind of the CRF emission source. The zone was positioned between 150 m and 300 m in a radial downwind of the emission source and the flight track (sampling area over the ground) was defined to be perpendicular to this radial with a width of up to 100 m, marked by high visibility cones to act as a guide to the pilot and a warning to others on site (as briefed). This width was deemed sufficient to fully capture the plume morphology based on visual inspection of a smoke flare released prior to the experiments from the points of release. Conceptually, the required width would be expected to increase as distance between downwind sampling and source increases.

Each flight of the tethered rotary UAS was conducted by two personnel - a pilot and an observer. The pilot was in overall charge of the UAS, while the observer was responsible for monitoring any emergent hazards to the flight, including communicating with other personnel on site. A third scientific observer was tasked with guiding the UAS sampling, which was conducted manually by the pilot.

After take-off, the pilot conducted vertical and lateral sampling manually within the pre-defined zone, ensuring that both in-plume and out-of-plume measurements were recorded. The out-of-plume measurements were important to define the background conditions needed for the mass balance flux calculation (discussed further in section 5).

Each flight lasted between 17 and 28 minutes, constrained by the UAS battery charge, which was monitored by the pilot and observer team.

Seven rotary UAS flights were conducted which measured emitted CH_4. The times of these flights, wind conditions (as measured by on-site 2 m elevated sonic anemometers) and the corresponding CRF release configuration are given in Table 4.2.

Table 4.2 Time of UAS rotary flights, mean wind direction and speed (to 3 significant figures), and corresponding release configuration (as defined in Table 4.1)

Flight number	Date and time	Release number	Wind speed and direction
1	2/11/16, 16:03 to 16:22	8	1.45 m/s, 309°
2	3/11/16, 11:17 to 11:46	9	3.81 m/s, 234°
3	3/11/16, 11:52 to 12:17	9	3.84 m/s, 233°
4	3/11/16, 14:33 to 14:55	10	4.39 m/s, 232°
5	3/11/16, 15:03 to 15:25	10	3.70 m/s, 226°
6	3/11/16, 15:46 to 16:07	11	3.05 m/s, 224°
7	3/11/16, 16:19 to 16:41	11	2.06 m/s, 202°

5. Results and Discussion

This section discusses the flux results and overall validation of the UAS mass balance method in the series of experiments described in section 4. An example flight is presented in detail to illustrate typical UAS sampling and the flux-calculation method. The results are also compared with those obtained using a complementary measurement technique based on the tracer dispersion method reported in Appendix E.

5.1. Data illustration for an example flight

The results for Flight 4 (see Table 4.2), which was conducted on the afternoon of 3 November 2016 under conditions of moderate wind (4.39 m/s) from the south west (232°), are presented here as an illustration of the data gathered.

Figure 5.1 shows the horizontal (latitude, longitude) flight track of the UAS for this flight, which shows the choice of a general orientation for the sampling perpendicular to the mean wind direction, which was from the southwest. This orientation defines the flux plane used in the mass balance method. The end-points of the flight track were converted to relative distance (or range) using spherical trigonometry (as units of longitude and latitude vary sinusoidally with latitude). This was then used to define the angle of orientation of the sampling plane relative to the mean wind direction recorded over the flight, in order to evaluate the perpendicular wind speed component from the measured wind speed and direction, as needed for Equation 1.

As the flight was piloted manually, we can see some variability (<6 m) around the mean orientation of the flux plane (seen as the non-zero minor-axis width in Figure 5.1). As Equation 1 does not implicitly require that the flux plane is equidistant from the source, this is not expected to manifest an additional source of error. However, dilution and dispersion effects might be expected to result in systematic error in measured concentration if this distance varied significantly. In this example, the flight was >200 m from the emission source, such that the maximal variance in the distance of the flux plane from source is less than 3% of the distance from source, which is considered negligible. In addition, as the variability in distance from source is generally symmetric around the axis of the mean flux plane used, any effect can, in principle, be expected to largely cancel out. Use of pre-defined way-points and automated sampling (by autopilot) could remove any potential for this error source entirely as rotary UAS GPS station-keeping can be better than a few centimetres, even under strong and/or turbulent wind conditions.

Figure 5.1 The horizontal (latitude, longitude) flight track of the rotary UAS for Flight 4
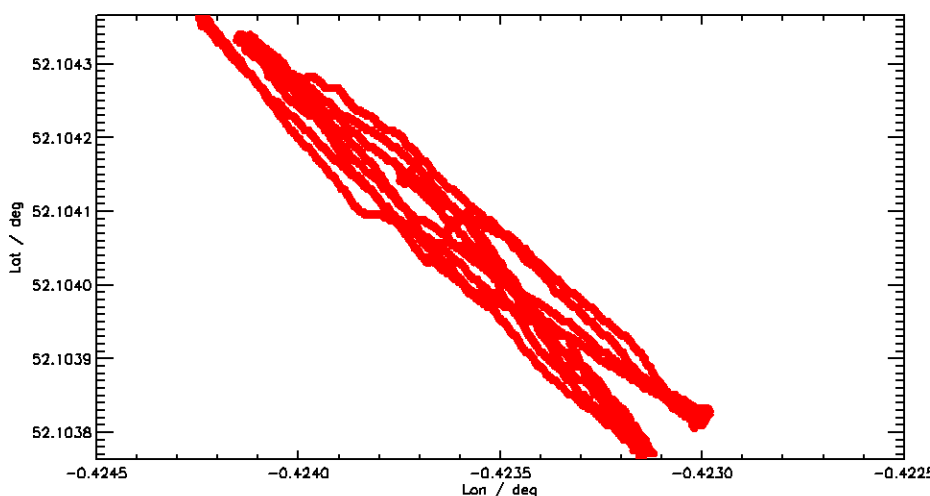
Figure 5.2 shows the measured CH_4 concentrations with time during the flight. The plot clearly shows the times when the UAS intercepts and samples the emitted plume, and periods where the UAS is clearly outside of the plume and sampling background air (characterised by CH_4 concentrations of ~2 ppm).

Figure 5.2 Time series of sampled CH₄ concentrations for Flight 4
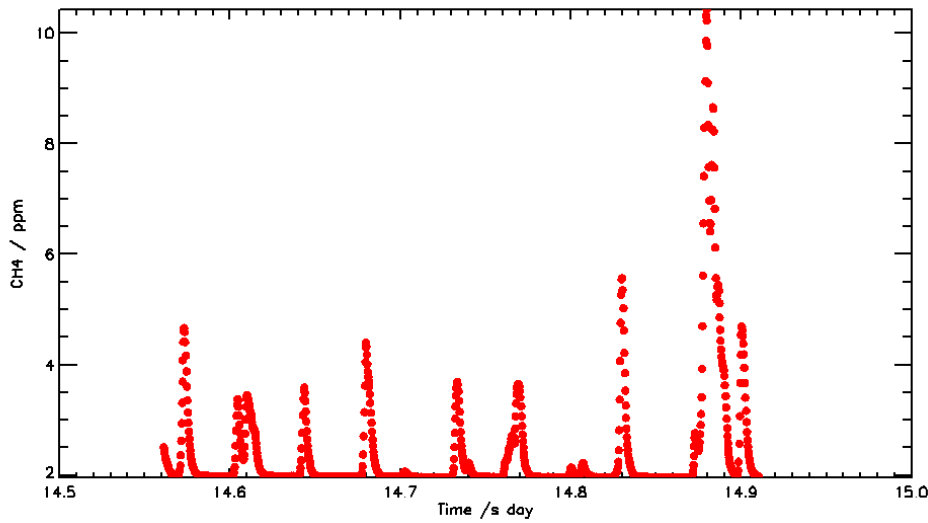
The X-axis units are fractional hours (Universal Time)

Figure 5.3 shows the UAS sampling in the vertical horizontal domain, colour-scaled for instantaneously measured CH_4 concentration, ranging from background concentrations (~1.95 ppm) to 10.4 ppm (seen in red). What we can start to see in this figure is the width and location of the central plume (seen in the lighter blue colours between 30 and 70 m range and 0 and 20 m height). These lighter blue colours correspond to concentrations between 4 and 6 ppm (or two to three times typical background concentrations). Such concentrations are typical of those sampled in landfill environments.

Figure 5.3 Horizontal/vertical flight track, colour-scaled (as per scale bar) for measured CH₄ concentration for Flight 4
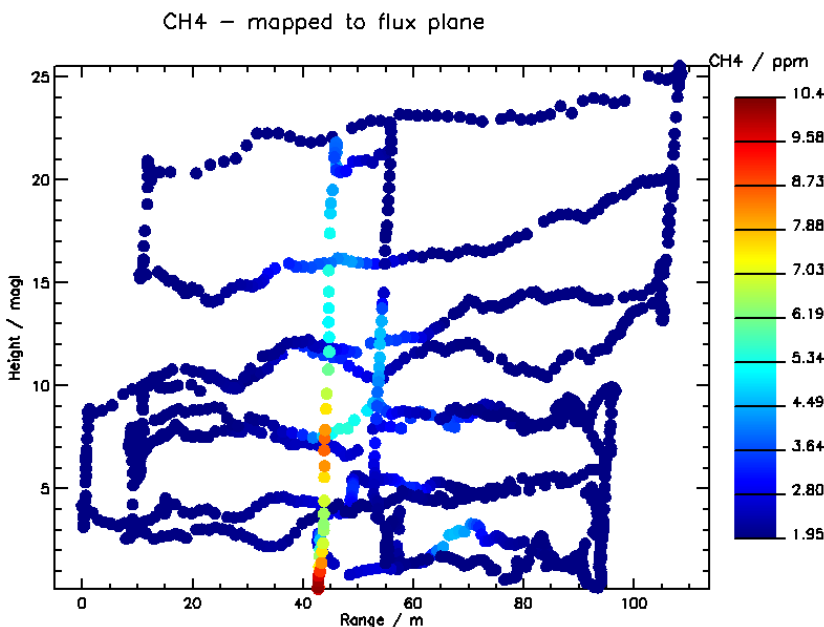
Figure 5.4 illustrates how the sampling in Figure 5.2 translates into averaged gridded (5 m × 5 m) flux cells, which very clearly highlights the plume morphology and footprint within the broader flux plane. These flux cell averages (and their corresponding standard deviations) are then integrated using Equation 1 and convolved with the mean wind speed measured across the flight to derive the total CH_4 flux, while flux uncertainty is calculated from Equation 2 using the sampled (or known) statistical errors (or variability). The mean wind speed and direction were calculated from

one-minute averages of a Met Office sonic anemometer data placed on a 5 m tower in the centre of the Cardington site.

Figure 5.4 CH₄ concentrations gridded (averaged into 5 m cells) across the flux plane, coloured as per scale for Flight 4
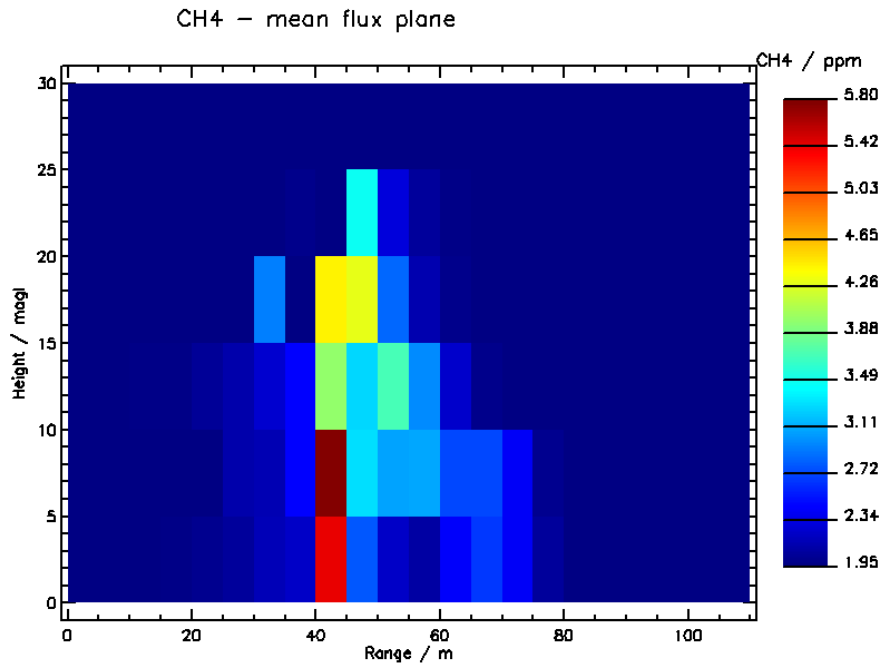
The gridded data (evaluated in the same way as the example here for Flight 4) from sampling for other rotary UAS flights can be seen in Appendix C.

5.2. Flux validation results

The resulting UAS-derived mass balanced fluxes and their comparison with CRF fluxes are presented in Table 5.1 for the seven flights. The CRF flux tolerances in Table 5.1 represent a maximum error, while the UAS flux tolerances represent a one standard deviation uncertainty calculated using Equation 2.

The range of the one standard deviation uncertainties on the mass balance fluxes always overlaps with the corresponding mean CRF flux and often overlaps very well, with a least squares correlation coefficient across all flights of 0.95. We can therefore be confident that the uncertainty budget defined by Equation 2 performs well in accurately capturing and representing the sources of uncertainty in the measurement and forward model.

The minimum relative bias is seen to be 0.1% (Flight 5), while the maximum relative bias is 39.6% (Flight 6), though the bias for the latter flight is calculated relative to a smaller emitted flux, so relative error is amplified. Absolute biases range from 0.1 kg/h (Flight 5) to 2.6 kg/h (Flight 3).The mean percentage bias for these 7 flights is +5.7% and the absolute mean flux bias is +0.42 kg/h, with a standard error on the mean flux of 1.07 kg/h (across the seven flights), which corresponds to less than 10% of the mean flux.

Table 5.1 CRF flux and UAS-derived mass flux (and flux uncertainty) comparison data and bias

Flight number	UAS flux (kg/h)	Release number	CRF flux (kg/h)	Mean flux bias (kg/h) (and bias %)
1	9.3 ± 2.7	8	10.9 ± 0.5	-1.6 (-14.7%)
2	12.8 ± 2.6	9	10.9 ± 0.5	+1.9 (17.4%)
3	13.5 ± 2.4	9	10.9 ± 0.5	+2.6 (23.8%)
4	9.5 ± 1.5	10	10.9 ± 0.5	-1.4 (-12.8%)
5	11.0 ± 2.3	10	10.9 ± 0.5	+0.1 (0.1%)
6	7.4 ± 2.0	11	5.3 ± 0.2	+2.1 (+39.6%)
7	4.6± 0.7	11	5.3 ± 0.2	-0.7 (-13.2%)

All values are rounded to 1 decimal point

5.3. Additional considerations

A range of analytical tests were carried out by the team to evaluate the flux calculation method within the sampling constraints.

5.3.1. Grid spacing

As discussed in section 2.2, it was found that the choice of grid spacing is, in practice, a compromise between the representative length scale of the measurement by the instrument and the need to avoid including dead space in the flux plane, which could otherwise act to bias the true result.

A range of grid cell lengths was tested for all flight experiments here, from 1 to 20 m. That analysis found that grid cells less than ~5 m resulted in fluxes that were systematically and consistently biased low (due to the fact that such small length scales do not represent the measurement at typical wind speeds), while length scales greater than 20 m were often systematically biased high due to the inclusion of a larger proportion of dead space. In most flights, a "plateau" in calculated fluxes was observed between approximately 5 m to 15 m, representing an optimal balance between spatial representation of the data and unwanted dead space. In practice, the bounds of this optimised grid spacing is defined as a function of the wind speed and the coverage of the flux domain. For example, a choice of 5 m (as used in this analysis) is appropriate for wind speeds ranging from 1 to 5 m/s for the UGGA instrument (with a response time of 1 s). However, for instruments with faster (or slower) response times, a smaller (or larger) grid spacing may be required. Ideally, an analytical approach such as that described above would be required to determine an acceptable range for each flight. However, the experiments above suggest that as long as there is sufficient, and equal, sampling across the flux domain, a rule of thumb for an appropriate grid spacing remains equal to the product of mean wind speed (perpendicular to the flux plane) and characteristic instrument response time.

5.3.2. Normalisation

A further test was carried out to test sensitivity to weighting grid cells for their relative sampling (also known as normalisation). For all but Flight 6, this had only a marginal effect on the final flux (no more than a 5% difference). However, normalisation can act to amplify any effect due to non-randomised sampling of the flux domain if such sampling is not carefully conducted. As flights were carried out manually here, this could not be robustly ensured and so normalisation has not been applied to the gridded flux data. However, as guidance, normalisation could be a useful additional part of any flux algorithm as long as regularised sampling is conducted (e.g. by autopilot programming).

5.3.3. Sampling extent

A further consideration concerns the length of time (or sampling) that is required to build acceptable statistics for flux precision. In principle, the statistical accuracy of the calculated flux should improve with greater sampling time (for a static emission source). Gaussian statistics imply that the standard mean error on the flux should scale inversely with the square root of the number of samples. In practice, the statistical uncertainty on flux is more complicated in our application here as spatial sampling is also important and the standard mean error instead scales with the convolution of the number of samples in each flux grid square in the flux domain and the total number of grid squares in the domain. In the error propagation model defined earlier, we can define the uncertainty in each experiment analytically. The experiments conducted here do suggest that ~20 minutes of flight time (for a precision instrument sampling at 1 Hz) is sufficient to derive flux accurate to within 40% for a point source when measuring 100-300 m downwind for a mean wind speed of ~2 m/s. In practice, this uncertainty can only be used as a rough guide as the true statistic is experiment-specific and is a function of both spatial sampling and external factors such as wind speed and wind speed variability, the latter of which can increase significantly in stagnant (turbulent) flow regimes. For example, this uncertainty would be reduced for less variable winds and high atmospheric stability. However, a landfill plume may be expected to be wider than the landfill area itself, requiring a larger flux domain than that required here, thereby reducing the sampling density for equivalent time. However, it is possible to define a minimum sampling time using the rule of thumb that Gaussian statistics require at least 50 measurements per grid cell and evaluating the time it would take to fill a pre-defined flux domain downwind of a landfill source. For example, a 200 m wide plume, which may be expected to rise no more than 50 m in height by a point of measurement 300 m downwind, would require at least 42 minutes of continuous sampling (for a 10 m grid spacing and 2 m/s wind speed) to achieve similar statistics to those derived in Table 5.1, with additional sampling required out of plume to sample background variability. This also assumes that the UAS is continually moving at constant velocity through the flux domain to achieve equal sample weighting, which could be facilitated by autopilot programming. Such a calculation could easily be conducted prior to site visits using forecast meteorology to determine the duty cycle of UAS sampling in a pre-defined flux domain. Additionally, simultaneous sampling upwind of a landfill source could yield background variability without the need to conduct out-of-plume sampling downwind, though this adds further complexity to the design of operational measurement.

5.3.4. Non-point source emissions

A further aim of our experiments was to diagnose the method's ability to derive flux from non-point sources, by using multiple release nodes from the CRF facility. Flight 5 was conducted for a release from an elevated node at 6.2 m (Release 9 in Table 4.1). A double plume was identified and mapped in the flux domain (see Appendix C, Figure C.5). This flight was conducted at our minimum distance from the CRF sources (~80 m), and consisted of two release nodes mounted 30 m apart horizontally. We clearly see evidence for 2 distinct plumes in the sampling in this flight at roughly the same distance apart downwind with summative emissions where the plumes appear to overlap. The fact that this configuration does not seem to have affected the accuracy of our flux calculation using the mass balance method supports the utility of UAS sampling and mass balancing for calculating bulk net emissions from diffuse sources such as landfill.

5.3.5. Wind speed and direction measurements

On flights where the wind was light (1- 2 m/s – corresponding to Flights 1 and 7), the wind direction was sometimes seen to be highly variable (due to near-surface turbulence), which can be expected to result in large uncertainties by Equation 2. This was the case in Flight 1 (represented by the high relative uncertainty seen in Table 5.1 for this flight). However, a less variable wind direction measured during Flight 7 (despite a relatively low wind speed), resulted in reduced overall uncertainty. Also, in turbulent conditions, such as those during Flight 1, it cannot be readily assumed that the wind speed in the flux plane is isotropic and representative of a remote (displaced) measurement of wind speed, especially if that remote wind measurement is subject to variability not likely to analogously impact the flux plane (e.g. due to nearby obstacles which disturb near-surface flow). There are two solutions that could help with this. First, and ideally, wind should be measured on-board the UAS itself (though this remains a challenge for rotary UAS due

to the flow disturbance by the rotors). Second, operational flux measurements should only be carried out for moderate wind speeds when flow may be expected to be more uniform in the near-surface environment and less variable (notwithstanding nearby obstacles or buildings).

5.3.6. Use of tethered inlet

The use of a tethered inlet system, which draws sampled air down from the location of the UAS to instrumentation on the ground is not optimal. Ideally, an instrument with equal measurement precision and accuracy would be mounted directly on the UAS to avoid the lag time associated with pumping air and the logistical and safety constraint concerned with ensuring that the tether is not snagged or kinked due to objects on the ground. Tests were conducted prior to, and after, every flight to measure the draw-down time of air in the 150 m Teflon inlet and this time was found to be 290 s (±5 s). As this time must be subtracted from the time of measurement by the UGGA instrument on the ground to derive the corresponding time (and therefore location) of the UAS when the air was drawn in aloft, any uncertainty in the draw-down time can manifest as an error in the position of the UAS at the time of the sample, thereby potentially impacting the flux calculation. Sensitivity tests were conducted to examine this source of uncertainty (or error) and only small changes in calculated flux were observed (<5% of total flux). This potential for error could be negated using very recently developed (lower weight) in situ precision instrumentation, simultaneously removing this additional logistical and flight safety consideration.

5.4. Suitability for other applications

The validation exercise here was conducted for point source emission rates of 5 kg/h and 10 kg/h of CH_4 gas. However, such rates may be significantly higher than fugitive emissions of CH_4 gas that may be expected from oil and gas infrastructure and other industrial activities, which may be of interest in terms of the transferrable monitoring potential of this technology. In this section, we briefly review this potential in the context of the validated measurements and potential limits of detection.

Optimally, a range of much smaller CRF flux rates would have yielded truly validated information on the limits of useful flux quantification using the mass balancing method. However, measurements of CO_2-only emissions by the NPL CRF facility are instructive for this purpose. These (CO_2-only) release experiments were conducted prior to the delivery of CH_4 gas on 2 November 2016. The CO_2 gas cylinders used for those experiments was known to contain a trace amount of methane gas (<0.02% by mass, according to BOC specifications, although we note that laboratory testing of such cylinders have been found to have much higher contaminant concentrations in the past)).

The mixing line (ratio of measured concentrations of CH_4 and CO_2) for a UAV flight experiment for a CO_2-only release is shown in Figure 5.5. The mass ratio of the measured gases (527) shows that we have calculated a 0.190% (to three significant figures) potential methane contamination of the CO_2 gas sampled downwind in the experiment. This offers a noteworthy limit of detection by our method, in that it demonstrates that the instrumentation is sensitive enough to detect even very small traces of contaminant gases in an otherwise relatively pure sample of another calibrant gas. A flux of (contaminant) CH_4 was derived for this experiment, yielding a CH_4 flux rate of 0.0422 g/s (0.151 kg/h, to three significant figures) with a one-standard-deviation flux uncertainty of 0.0105 kg/h (~24%). Thus, we can see that even for methane fluxes as small as 0.15 kg/h, we can still derive flux rates with similar relative uncertainties to those at methane flux rates over an order of magnitude higher (as used in the main methane release experiments). These small flux rates are similar in magnitude to the small point source emissions that may be expected from fugitive emission sources in natural gas infrastructure. We can therefore conclude that the method developed here may have significant utility in the monitoring and measurement of fugitive methane emission flux rates from other UK industrial infrastructure.

Figure 5.5 Scatter plot (mixing correlation line) and line of best fit for instantaneously-measured concentrations of CH₄ and CO₂ for a CO₂-only release experiment on 2 November
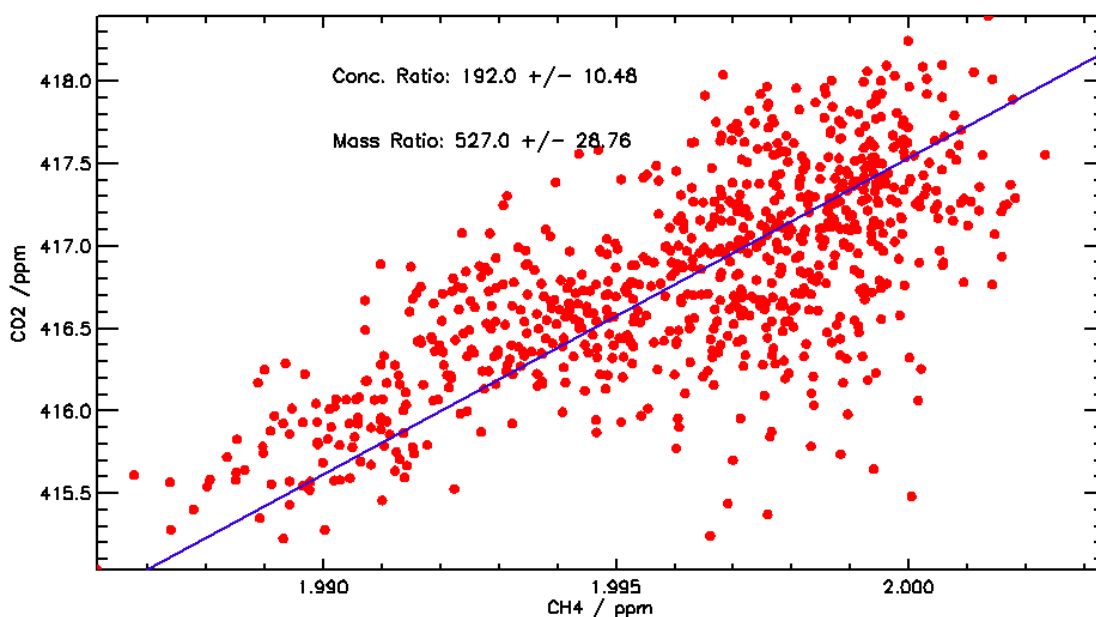
The line of best fit is shown in blue and the corresponding concentration and mass ratios of CO_2:CH_4 are shown in the panel together with the one-standard-deviation uncertainty derived from the mass balance flux method

5.5. Tracer dispersion method results

Independent Tracer Dispersion Method (TDM) validation experiments were carried out by the University of Southampton (UoS) and the Technical University of Denmark (DTU) alongside the UAS validation.

TDM combines a controlled release of tracer gas at the CH_4 emission source (e.g. from a landfill), with CH_4 and tracer concentration measurements downwind of the CH_4 source using a mobile high-resolution analytical instrument. The method is based on the assumption that a tracer gas released on a landfill will disperse in the atmosphere in the same way as CH_4 emitted from the landfill will disperse. Assuming a defined wind direction, well-mixed air above the landfill (causing the emitted CH_4 and released tracer gas to be fully mixed), and a constant tracer gas release rate, the CH_4 emission rate can be calculated as a function of the ratio of the integrated cross-plume concentration of the emitted CH_4 and the integrated cross-plume concentration of the released tracer gas.

Five TDM validation tests (four for DTU) were carried out alongside the UAS validation experiments using C_2H_2 as the tracer gas. The release rate (mass flux) of the CH_4 was controlled and regulated by NPL, but not known to either monitoring team at the time of the experiment or during the initial analysis of data. Likewise, monitoring data was not shared or discussed between the monitoring teams until after data had been analysed. A comparison between derived flux and actual flux was made only after the conclusion of the project.

Full details of the experimental setup, data processing and results are given in Appendix E. Table 5.2, shows the average measured CH_4 fluxes for each release compared to the actual CH_4 flux rate.

Table 5.2 Methane flux measurements

CRF release number	Actual flux (kg/h)	UoS flux (kg/h)	DTU flux (kg/h)	UAS flux (kg/h)
8	10.9 ± 0.5	10.4 ± 0.5	9.86 ± 2.2	9.3 ± 2.7
9	10.9 ± 0.5	11.9 ± 3.8	10.39 ± 3.3	12.8 ± 2.6 and 13.5 ± 2.4
10	10.9 ± 0.5	10.6 ± 1.3	11.22 ± 2.7	9.5 ± 1.5 and 11.0 ± 2.3
11	5.3 ± 0.2	5.4 ± 0.7	4.34 ± 0.3	7.4 ± 2.0 and 4.6 ± 0.7
12	10.9 ± 0.5	12.0 ± 3.6	-	-

5.6. Method and results comparison

Table 5.2 indicates that both the UAS and TDM techniques were able to determine actual release rates to within one standard deviation of the measurement uncertainties for each test.

The two methods have different operating constraints that potentially makes the techniques highly complementary. This is summarised in Table 5.3.

Table 5.3 Operational constraints

Potential Constraint	UAS	TDM
Access	Area of dimensions 200 m by 200 m within 1 km of the source to fly UAS. Must be >150 m away from people, buildings, roads or cattle not under the direct control of the pilot	A network of roads or tracks 1 to 6 km downwind of site, preferably perpendicular to the wind direction
Interference from external CH_4 sources	A tractable problem under Equation 1, so long as the background CH_4 concentrations statistics can be robustly evaluated	Depending on wind direction this can cause problems
Terrain	Buildings and obstacles can perturb air flow, which can affect the precision of mass balance calculation due to wind variability in Equation 1. Flat fetch should be optimised for each site	Complex topography may influence interpretation of data
Meteorological conditions	UAS cannot operate when wind speed > 10 m/s, during inclement weather and during visibility <200 m, or at night	Wind speed generally above 2 m/s. High wind speeds may cause excessive dilution of source and tracer. Plume needs to ground off-site, which may not occur when high sensible heat fluxes occur (middle of hot sunny summer day). Night time tests good
Monitoring period	Duration of monitoring periods may be restricted by flight times (due to battery availability) and pilot fatigue. A single pilot crew may typically provide no more than 3 hours of operational flying/sampling per day	Duration of monitoring restricted to mass of tracer gas available
Health & Safety	Operation of a UAS requires training and CAA-recognised-provider training and certification for any commercial use. All UAS operation must comply with CAA regulations to protect public safety and property	Use of flammable gases

6. Recommendations and conclusions

6.1. Validation experiments

The validation experiments carried out for this project have successfully characterised the expected performance of a UAS mass balancing method for the derivation of fugitive CH_4 emission flux from landfills or other sources of CH_4. A total of seven flights were analysed, which sampled CH_4 concentrations from a UAS platform downwind of a controlled emission source with a known flux. Calculations of mass balanced fluxes were conducted blind prior to comparison with the controlled releases (see Table 5.1).

The key results of the validation experiments were as follows:

- The percentage difference between the calculated and emitted flux across all flights ranged from 0.1 to 39.6%

- Absolute difference ranged from 0.1 to 2.6 kg/h.

- The one standard-deviation uncertainties on the calculated flux overlapped with the corresponding emitted flux for each of the seven experiments.

- The least squares correlation coefficient between the calculated and emitted methane flux for all of the seven experiments was 0.95.

- The uncertainty budgeting algorithm described in Section 2.3 performs consistently well in accurately capturing and representing the sources of uncertainty.

- The mean percentage difference for the seven flights was +5.7% with a mean flux bias of +0.42 kg/h,

- The standard error on the mean flux was 1.07 kg/h corresponding to less than 10% of the mean flux.

6.2. Operational recommendations

The mass balancing method can be used for flux calculation from downwind sampling of an emission plume when:

- Sampling is (ideally) equally weighted across the flux plane, which must completely encompass the maximum extent of the plume.

- Sampling is not significantly unequally weighted to sample only the expected locations of the plume.

- Sampling frequency and total sampling time are sufficiently high, or long, respectively, such that the flux plane is sampled repeatedly to capture the time-varying footprint of the plume.

The following conclusions can be made regarding the expected operational performance of the method:

- The flux derived using mass balancing for each flight can be considered to be accurate within the range of the derived one standard deviation uncertainty, when all sources of variability and error required for the error propagation model (Equation 2) are known (or measured).

- Repeated flights (or increased sampling time) can serve to reduce the uncertainty envelope on the flux significantly, as long as the system can be assumed to be static. However, the sampling required to reach an arbitrary threshold of expected percentage uncertainty is a function of the local conditions and cannot be predicted prior to measurement.

- Sampling when the wind speeds, wind directions, and background concentrations are constant will lead to reduced uncertainty. In this analysis, variable wind direction (often coincident with low wind speeds) resulted in the largest uncertainty component in Equation 2.

- A characteristic typical uncertainty cannot be supplied for the method as each analysis will yield its own representative error - each flight (or analysis) will be subject to local variability (especially with regard to wind speed, wind direction, and background concentrations). However, a conservative maximum uncertainty from this series of experiments suggests that even for highly variable wind conditions such as those observed in Flights 4 to 7 (and when sampling concentrations typical of CH_4 levels seen downwind of UK landfills), the relative error may be no more than ~50% (at the 90% confidence level, equivalent to 1.645 standard deviations).

- Further improvements to the accuracy of flux calculation could be made by appropriate measurement of wind speed and direction on board the UAS, taking care to ensure that the UAS itself does not perturb ambient flow. In the absence of this, a nearby wind measurement on an elevated tower (preferably at 10 m above local ground level) remains a good substitute as long as this is placed in an analogous environment to the intended UAS sampling, that is, free from obstruction or perturbations to air flow that are not also expected in the UAS sampling area.

Future operational flux calculations should always require a site-specific (and UAS-instrument-specific) plan, for the following:

- Appropriate zoning of downwind areas to ensure that the sampling captures the landfill plume.

- The positions of obstacles to air flow (for example any buildings) and site topography between the site and measurement location should be noted and considered when planning UAS sampling to optimise the sampling zone to minimise any unwanted effects that may result if measurements are recorded nearby to such features.

- The locations of any nearby CH_4 emission sources that are not attributable to the target quantity (i.e. landfill site) must be noted. Ideally, these should not be upwind of the site of interest relative to the sampling area as this would greatly affect background variability and could result in much larger systematic errors. If this is unavoidable, additional care may be needed to ensure good background measurements are recorded to better remove the extraneous source.

- A grid cell spacing that represents the length scale of each independent concentration measurement, defined by the instrument response rate and the expected (or known) wind speed.

- Randomised but equal sampling of the entire flux domain, for a time needed to fill each grid cell with at least 50 independent CH_4 concentration measurements.

- Sampling in non-stagnant wind speeds (greater than nominally 2 m/s) to reduce flux uncertainty due to turbulent variability, with the upper limit defined by the safe operating conditions of the UAS.

6.3. Conclusions

The project has successfully tested the UAS method for quantifying methane from landfills emissions. The sources of uncertainty are known and can be quantified in future measurements. The key operational requirements for undertaking sampling have been identified and are set out in this report. Using the information provided by this report will enable the UAS mass balance method to be applied at UK landfills to quantify methane emissions.

The small methane flux rates detected in the carbon dioxide releases are similar in magnitude to the small point source emissions that may be expected from fugitive emissions in natural gas infrastructure. The method demonstrated here may therefore be useful for the monitoring and measurement of fugitive methane emission flux rates from other UK industrial infrastructure.

The tracer gas dispersion method was also successful in matching the known methane releases. The UAS and the tracer gas dispersion method have different operational constraints so together they represent different options that allow methane emissions from landfills and other facilities to be quantified within a known level of uncertainty.

References

ALLEN, G., HOLLINGSWORTH, P., ILLINGWORTH, S., KABBABE, K. AND PERCIVAL, C. (2014) *Feasibility of aerial measurements of methane emissions from landfills*. SC130034/R. Bristol: Environment Agency.

ALLEN, G., PITT, J., HOLLINGSWORTH, P., MEAD, I., KABBABE, K., ROBERTS, G. AND PERCIVAL, C. (2015) *Measuring landfill methane emissions using unmanned aerial systems*. SC140015/R. Bristol: Environment Agency

CAA (2015) *Air Navigation : The Order and the Regulations*. CAP 393, 4th edition, 10 January 2015. London: Civil Aviation Authority.

IPCC (2007), *Climate change 2007 – The scientific basis*. Contribution of Working Group 1 to the Fourth Assessment Report of the Intergovernmental Panel on Climate Change. Cambridge University Press.

MAYS, K. L., SHEPSON, P. B., STIRM, B. H., KARION, A., SWEENEY, C. AND GURNEY, K.R. (2009). Aircraft-based measurements of the carbon footprint of Indianapolis. *Environmental Science & Technology*, 43 (20), 7816-7823.

MYERS, D. E. (1991). Interpolation and estimation with spatially located data. *Chemometrics and Intelligent Laboratory Systems*, 11 (3), 209-228.

Acknowledgements

List of abbreviations

CAA - Civil Aviation Authority

CRF - Controlled Release Facility

DTU - Technical University of Denmark

LGR – Los Gatos Research

MFC - Mass flow controller

NPL - National Physical Laboratory

OA-ICOS - Off-Axis Integrated Cavity Output Spectroscopy

TDM – tracer dispersion method

UAS - Unmanned Aerial System

UGGA - Ultraportable Greenhouse Gas Analyser

UoM – University of Manchester

UoS – University of Southampton

Appendix A – NPL Controlled release facility

The controlled methane (CH_4) and carbon dioxide (CO_2) gas source was created utilising the National Physical Laboratory (NPL) Controlled Release Facility (CRF), which has been developed to meet the need to effectively simulate a broad range of real-world gaseous emissions scenarios. This allows the testing and validation of currently available and new monitoring techniques in the field by emitting selected gases at precisely controlled emission rates. For natural gas, composition was determined by calibration with NPL traceable primary reference gas mixtures. For CO_2, the composition value was obtained from the industrial gas provider's data sheet. For both gases, volumetric emission rate was determined by calibration using a high volume primary piston flow meter

The CRF technique can be summarised as the release of gaseous species at a defined rate and in a customised configuration (see Figure A.1). This was achieved by the use of a high flow gas control system and an assortment of release nodes. Incorporating thermal mass flow control (MFC) devices, the high flow gas control system consists of four primary flow channels, and two smaller channels, allowing for the addition of purge, cross-interfering, diluent or tracer gases into each primary channel if needed. The use of MFCs allows for the gas release rate to be precisely and accurately metered, as well as ensuring high repeatability and low levels of drift.

The facility was computer-controlled and monitored, allowing for the execution of pre-written operational programs and analysis of flow data post-test. Communication to the instrument was made via a low voltage umbilical cable allowing the operator to control the system from a distance of up to 50 m.

Emission source distribution was controlled by the use of several interchangeable nodes. Simple emission patterns were created by the use of an individual node, or up to four nodes used together to create more complex emission landscapes. Nodes were each connected to the blender using 75 m distribution hoses which allows for the distribution of sources over an area of up to 1 ha. Nodes consist of a 10 m flexible line source, a vertically orientated point source and four 0.65 m^2 diffuse area sources. Each primary flow channel had a full-scale range approximately equivalent to 30 kg/h CH_4 or 90 kg/h of CO_2.

Figure A.1 The CRF has previously been deployed to compare NPL DIAL capabilities (left). A CO_2 emission from a release node imaged via a gas imaging IR camera (right)
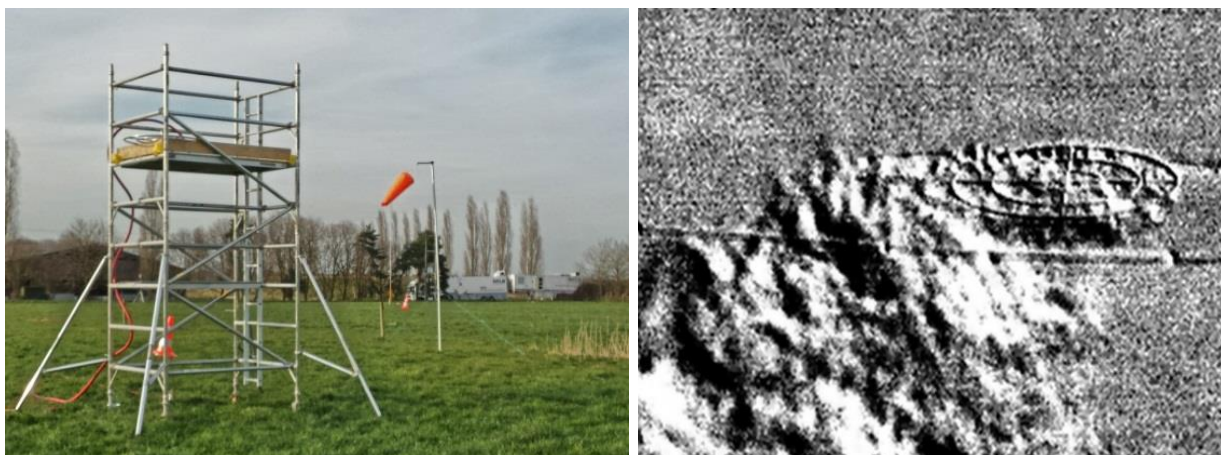
A series of controlled releases of CO_2 and natural gas was undertaken within the Met Office site at ground level, at the northeast corner winch hut rail and on elevated temporary scaffold platforms at ~6.2 m (Table A.1).

Table A.1 Controlled releases of CO_2 and natural gas

Release number	Remarks	Date and time (GMT)	Node position(s)	Flux rate (kg/h)
1	CO_2 release, single node, A, ground level release	1/11/16 13:28 to 13:43	A: 52.10461N, 0.42269W	A: 11.5 ± 0.4
2	CO_2 release, single node, A, top of NE winch hut rail.	1/11/16 14:53 to 15:12	A: 52.10422N, 0.42234W	A: 17.1 ± 0.5
3	CO_2 release, single node, A, top of winch hut rail	1/11/16 15:23 to 15:46	A: 52.10422N, 0.42234W	A: 17.1 ± 0.5
4	CO_2 release, single node, A, top of winch hut rail	1/11/16 16:03 to 16:29	A: 52.10422N, 0.42234W	A: 22.7 ± 0.7
5	CO_2 release, two nodes, A and C, ground based, release cut short.	2/11/16 10:24 to 10:33	A: 52.10466N, 0.42405W C: 52.10498N, 0.42331W	A: 8.7 ± 0.3 C: 8.3 ± 0.3
6	CO_2 release, two nodes, A and C, ground based.	2/11/16 11:24 to 11:42	A: 52.10466N, 0.42405W C: 52.10498N, 0.42331W	A: 8.7 ± 0.3 C: 8.3 ± 0.3
7	CO_2 release, two nodes, A and C, ground based	2/11/16 12:00 to 12:23	A: 52.10458N 0.42326W C: 52.10463N, 0.42267W	A: 11.5 ± 0.4 C: 11.4 ± 0.3
8	CO_2 and natural gas release, two nodes A and B respectively from top of tower (~6.2 m)	2/11/16 15:00 to 16:35	Co-located at top of tower A and B: 52.10498N, 0.42331W	A: 11.5 ± 0.4 *B: 10.9 ± 0.5 †B: 0.43 ± 0.02
9	CO_2 and natural gas release, two nodes A and B respectively from top of tower (~6.2 m)	3/11/16 10:31 to 12:19	Co-located at top of tower A and B: 52.10356N, 0.42474W	A: 11.5 ± 0.3 *B: 10.9 ± 0.5 †B: 0.43 ± 0.02
10	CO_2 and natural gas release, two nodes A and B respectively from top of tower (~6.2 m)	3/11/16 14:26 to 15:29	Co-located at top of tower A and B: 52.10343, 0.42419W	A: 11.5 ± 0.4 *B: 10.9 ± 0.4 †B: 0.43 ± 0.02
11	CO_2 and natural gas release, two nodes A and B respectively from top of tower (~6.2 m)	3/11/16 15:36 to 16:40	Co-located at top of tower A and B: 52.10343N, 0.42419W	A: 5.9 ± 0.2 *B: 5.3 ± 0.2 †B: 0.21 ± 0.01
12	Natural gas only, single node, B, ground level release	4/11/16 08:31 to 10:00	B: 52.10380N, 0.42391W	*B: 10.9 ± 0.4 †B: 0.43 ± 0.02

The reported expanded uncertainties are based upon standard uncertainties multiplied by a coverage factor k = 2, providing a coverage probability of approximately 95%.

A and C: The mass release rate of CO_2 attributed to the release of nominally pure CO_2. These figures (and associated uncertainties) are based on a primary measurement of flow and the CO_2 amount fraction value stated on the providers data sheet.

*B: The mass release rate of CH_4 attributed to the release of natural gas. These figures (and associated uncertainties) are based on a primary measurement of flow and the CH_4 amount fraction values (determined by GC FID & TCD, with comparison to primary traceable standards) of a sample of the natural gas.

†B: The mass release rate of CO_2 attributed to the release of natural gas. These figures (and associated uncertainties) are based on a primary measurement of flow and the CO_2 amount fraction values (determined by GC FID & TCD, with comparison to primary traceable standards) of a sample of the natural gas.

Appendix B – UAS specifications and instrument details

This project made use of the UAS infrastructure and instrumentation developed and used in SC140015 (Allen et al. 2015). We briefly describe them again here.

We used a rotary UAS platform for the validation of CH_4 flux in this project (Figure B.1). The DJI-S900 rotary platform performed vertical and lateral profiles within and across the emission plume downwind of the NPL CRF emission source. Ambient air was sampled via a 150 m Teflon inlet to a ground-based precision CH_4 (and CO_2) instrument.

The simultaneous CH_4 (and CO_2) tethered system consisted of our modified DJI-S900 hexrotor UAS flown as described in section 3 between the ground and 120 m height, and lateral distances of up to 80 m from a ground-station. The DJI-S900 was equipped with a 150 m length of Teflon tubing, through which ambient air was pumped and sampled air to a Los Gatos Research Ultraportable Greenhouse Gas Analyser (UGGA), which employs OA-ICOS technology to retrieve gas concentration in air. The UGGA instrument has a calibrated measurement accuracy of ~5 ppb at 1 Hz for CH_4 and 0.5 ppm for CO_2.

The tethered UAS system did not include a direct wind measurement. Wind measurements were recorded at the Met Office Cardington site by three-dimensional sonic anemometers installed at various heights on towers across the field site operated by the UK Met Office. We used wind measurements recorded at 5 m above ground level for representative wind measurements in this experiment.

Figure B.1 The University of Manchester Tethered S900
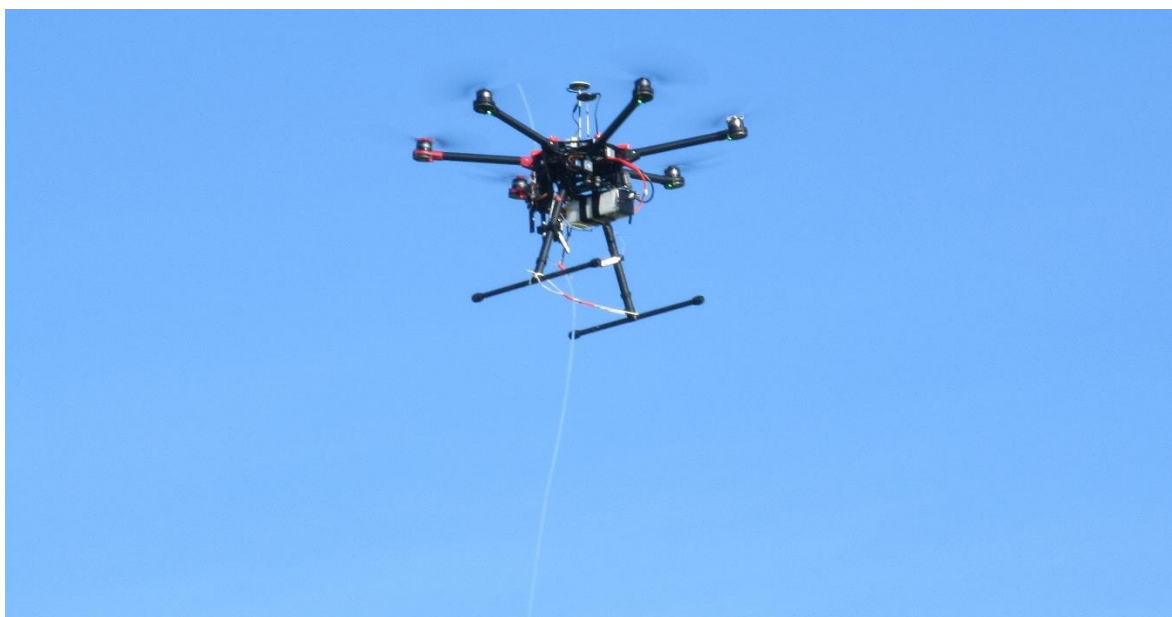
Airframe	Manufacturer	DJI
	Model	S900
	Take-off weight	5.5 kg (with 1 x battery pack) and 100 m of tubbing
	Propulsion	6 x 500 W electric motors
	Propellers	15 x 5.2 inches
	Main battery	1 x 6S 16 Ah
	Autopilot	DJI A2 controller
	GPS	DJI A2 GPS
FCS	Telemetry	None
	Command and control	2.4 GHz Futaba system
	Small logging computer	3DR PIxhawk (used for logging only)
Payload	Tubing	150 m of Teflon tube
	Sensor	Los Gatos Research (LGR) Ultraportable Greenhouse gas analyser (UGGA)

Appendix C – UAS measurement data

This appendix illustrates the sampling and gridded flux domains used for flux calculation for all seven rotary UAS sampling experiments listed in Table 4.2. In each case, a time series of measured CH_4 concentration in air and the gridded flux plane data are shown. These were then used to derive mass balance flux as reported in Table 5.1 in the same way as the example for Flight 4, as presented in section 5.1.

Flight 1

This experiment was conducted for a release from an elevated node at 6.2 m (CRF Release 8 in Table 4.1). A single plume was identified and mapped.
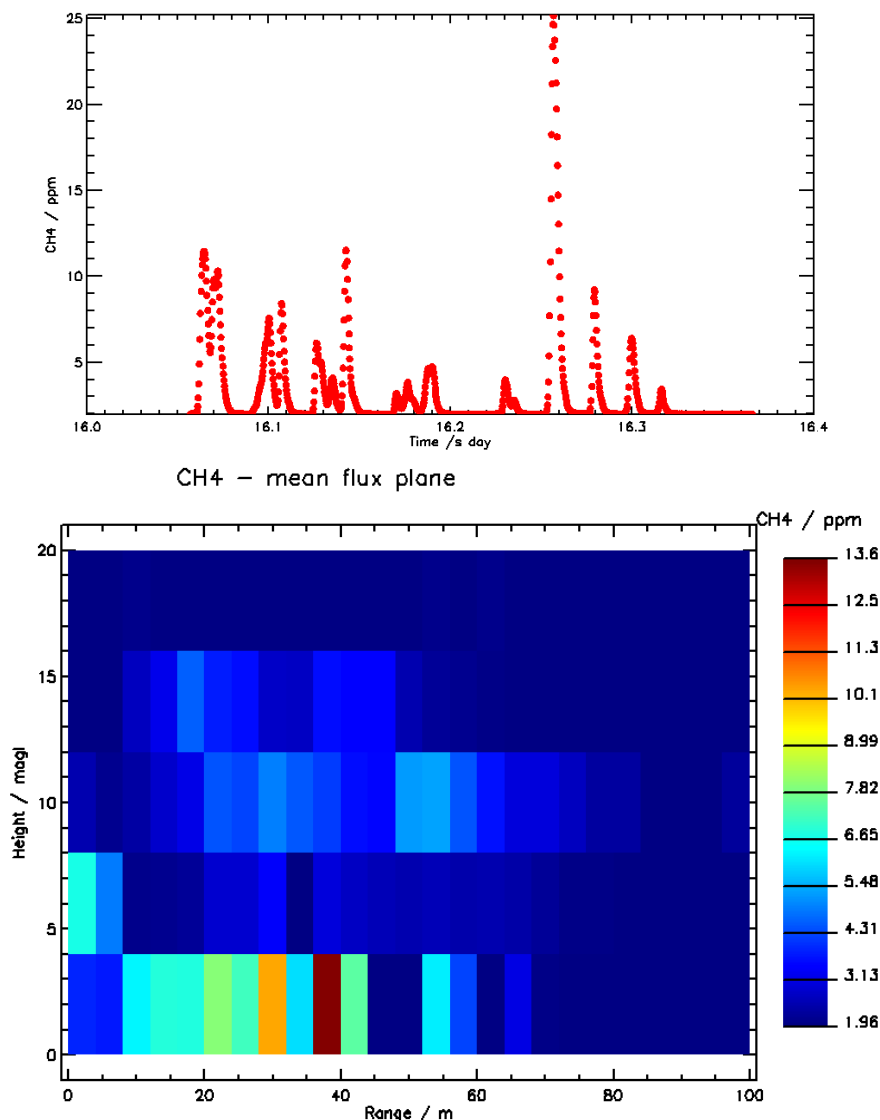
Figure C.1 Time series for Flight 1 (top panel) and gridded flux plane average concentrations (bottom panel)

Flight 2

This experiment was conducted for a release from an elevated node at 6.2 m (CRF Release 9 in Table 4.1). A single plume was identified and mapped in the flux domain.
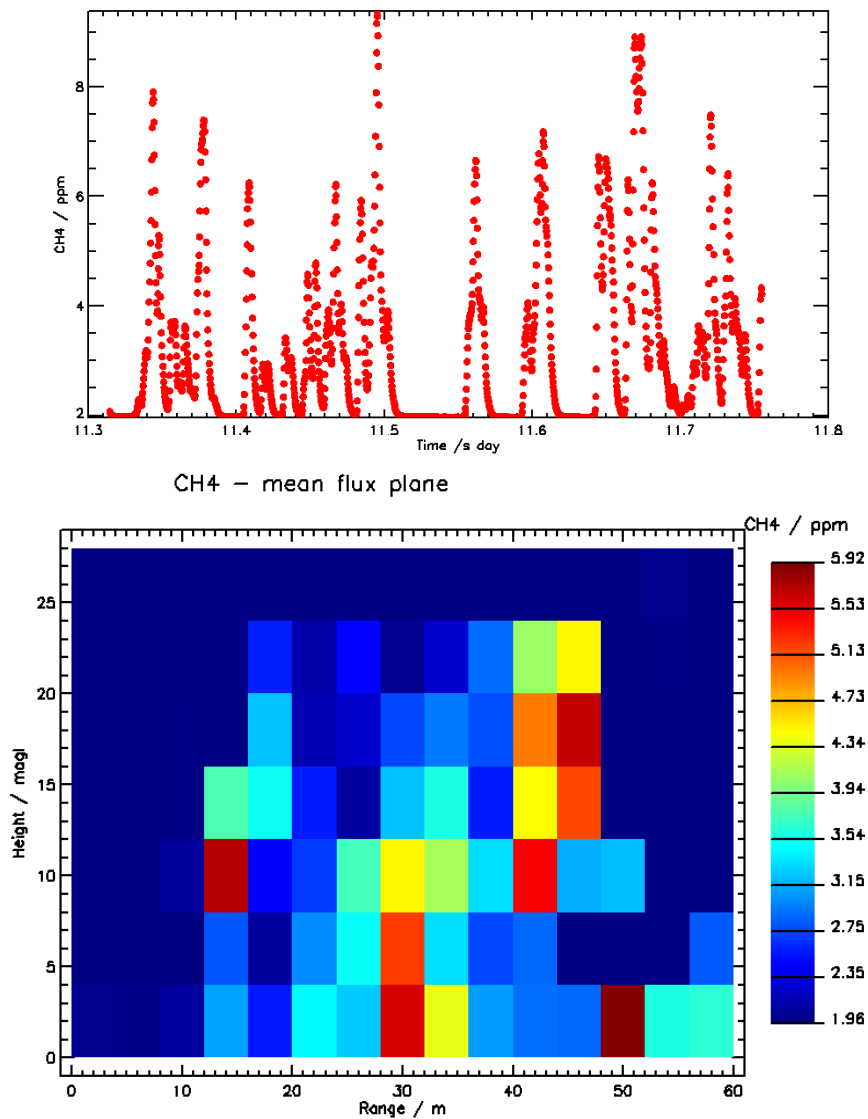
Figure C.2 Time series for Flight 2 (top panel) and gridded flux plane average concentrations (bottom panel)

Flight 3

This experiment was conducted for a release from an elevated node at 6.2 m (CRF Release number 9 in Table 4.1). A single plume was identified and mapped in the flux domain, however a slight wind direction change was observed over the course of the flight, reflected in the apparent double footprint.
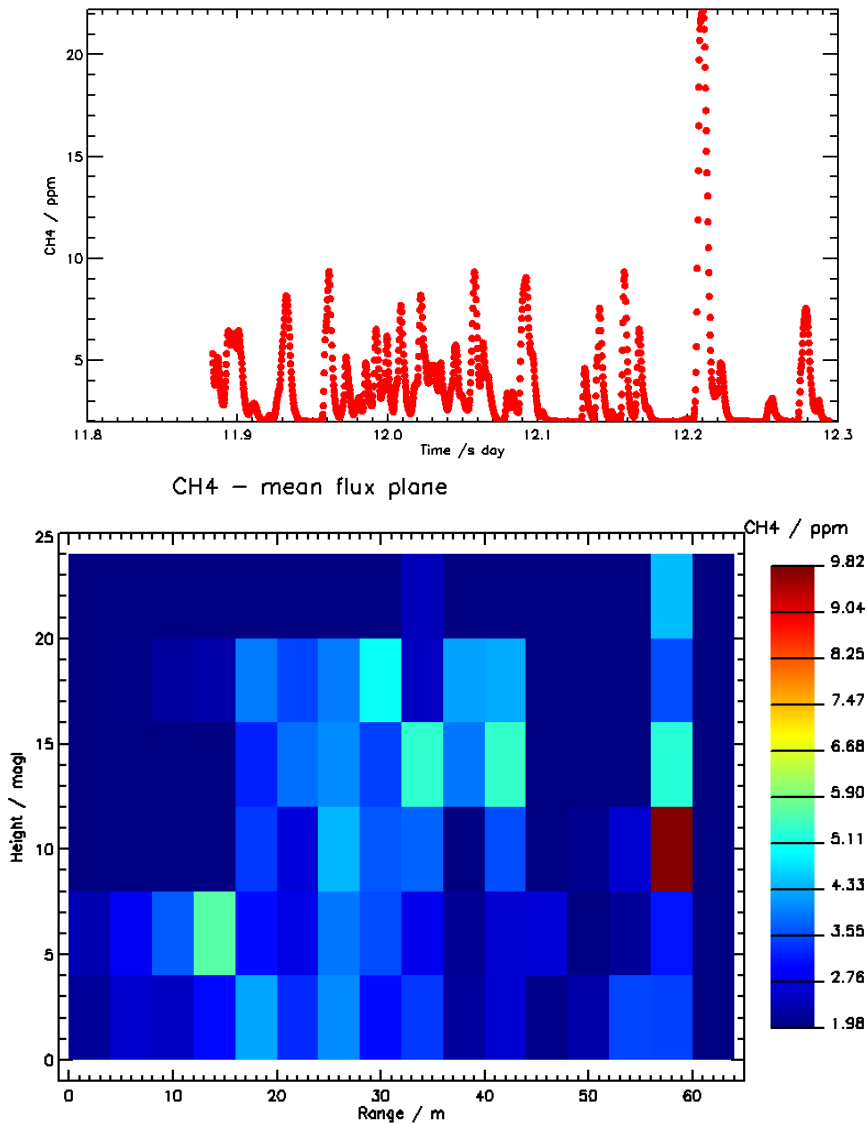
Figure C.3: Time series for Flight 3 (top panel) and gridded flux plane average concentrations (bottom panel)

Flight 4

This experiment was conducted for a release from an elevated node at 6.2 m (CRF Release 10 in Table 4.1). A single plume was identified and mapped in the flux domain.
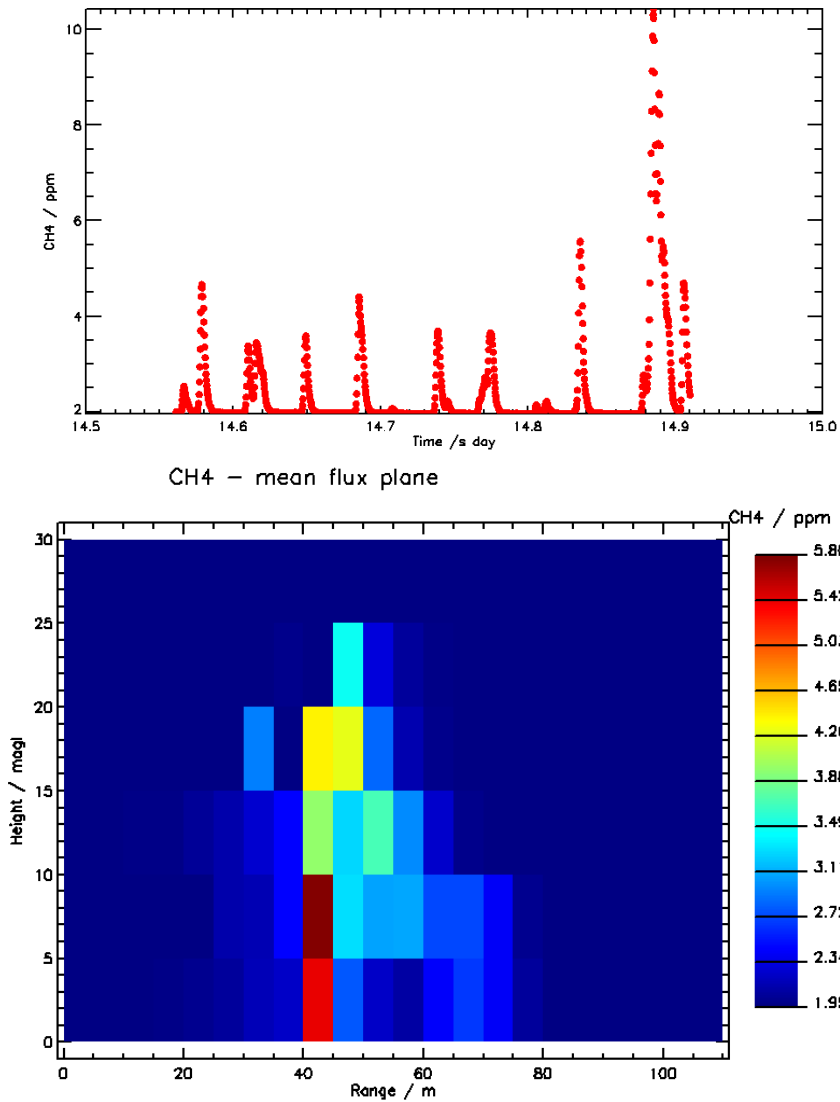
Figure C.4 Time series for Flight 4 (top panel) and gridded flux plane average concentrations (bottom panel)

Flight 5

This experiment was conducted for a release from an elevated node at 6.2 m (CRF Release 10 in Table 4.1). A double plume was identified and mapped in the flux domain. This flight was conducted at our minimum distance from the CRF sources, which consisted of two release nodes mounted ~ 30 m apart horizontally. We clearly see evidence for two distinct plumes in the sampling in this flight at roughly the same distance apart downwind with summative emissions where the plumes appear to overlap.
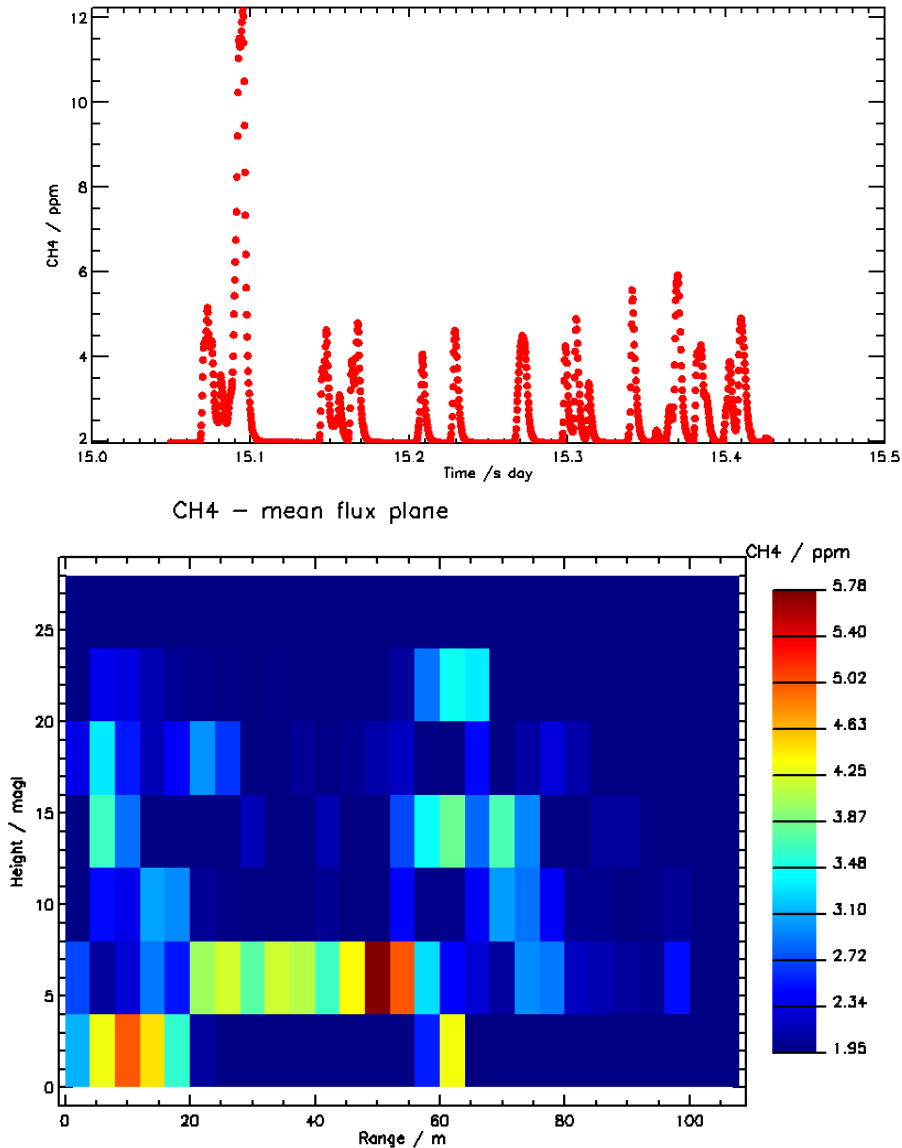
Figure C.5 Time series for Flight 5 (top panel) and gridded flux plane average concentrations (bottom panel)

Flight 6

This experiment was conducted for a release from an elevated node at 6.2 m (CRF Release number 11 in Table 4.1). A double plume was identified and mapped in the flux domain. This flight was conducted at our minimum distance from the CRF sources, which consisted of two release nodes mounted ~ 30 m apart horizontally. We clearly see evidence for two distinct plumes in the sampling in this flight at roughly the same distance apart downwind with summative emissions where the plumes appear to overlap.
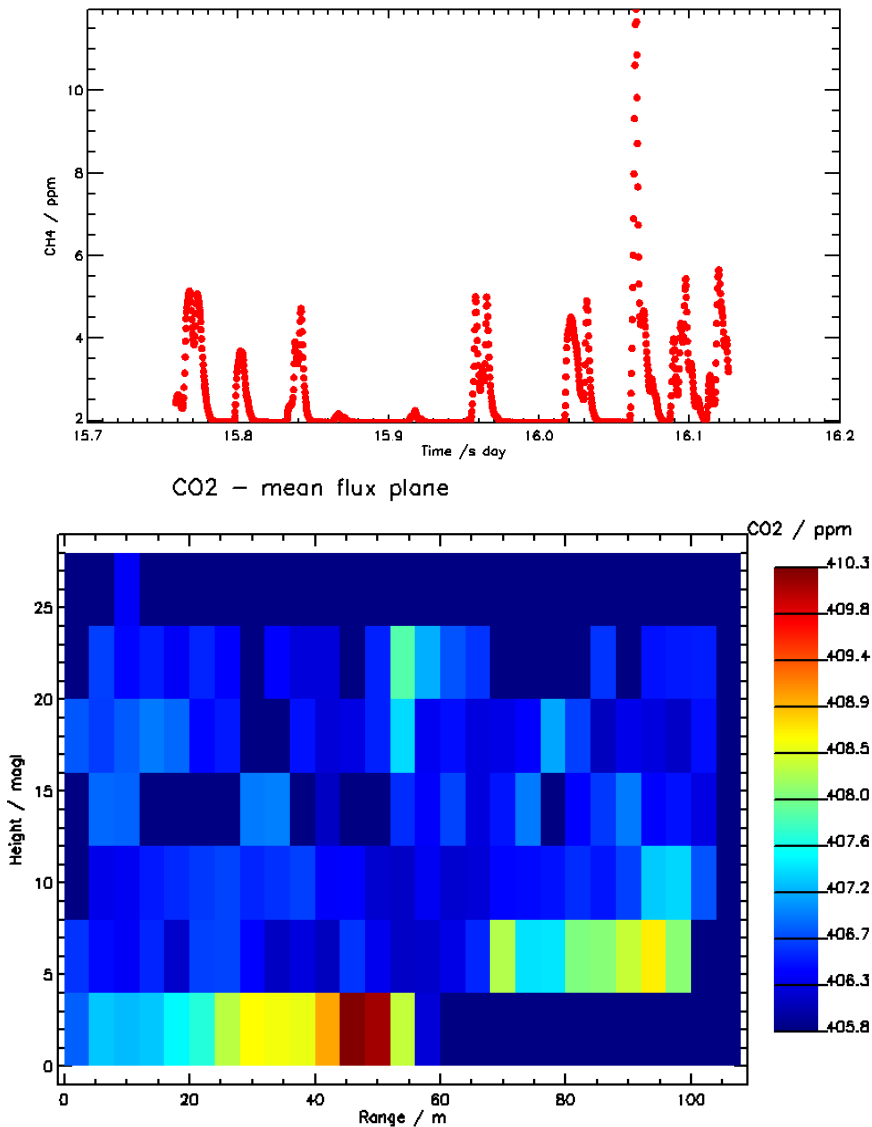
Figure C.6 Time series for Flight 6 (top panel) and gridded flux plane average concentrations (bottom panel)

Flight 7

This experiment was conducted for a release from an elevated node at 6.2 m (CRF Release 11 in Table 4.1). A double plume was identified and mapped in the flux domain. This flight was conducted at our minimum distance from the CRF sources, which consisted of two release nodes mounted ~ 30 m apart horizontally. We clearly see evidence for two distinct plumes in the sampling in this flight at roughly the same distance apart downwind with summative emissions where the plumes appear to overlap.
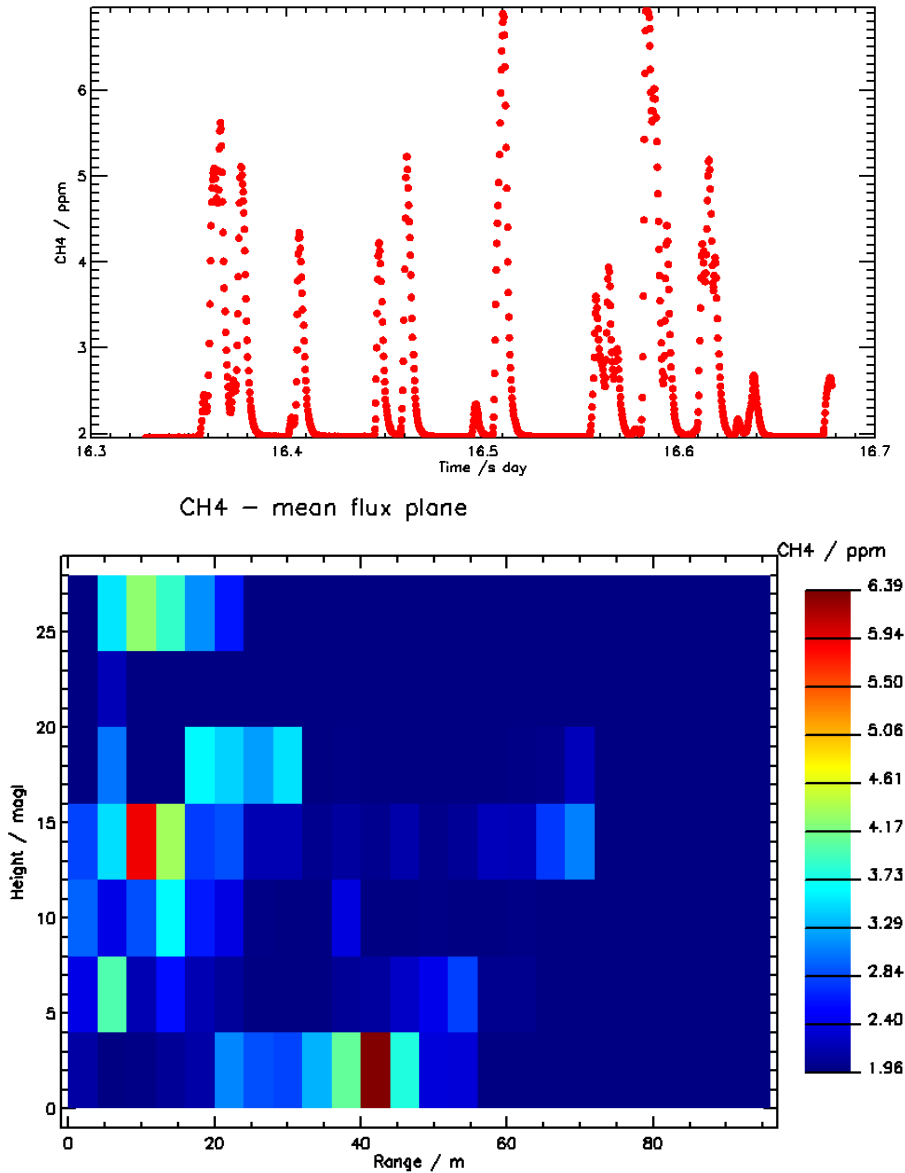
Figure C.7 Time series for Flight 7 (top panel) and gridded flux plane average concentrations (bottom panel)

Appendix D – Carbon dioxide measurements

In addition to the measurement of CH_4, we simultaneously measured CO_2 concentrations with the rotary UAS and UGGA system. The example below illustrates a rotary flight conducted on 3 November beginning at 11:17 (corresponding to Flight 2 in Table 4.2). In this experiment, both CO_2 and CH_4 were released from the CRF Facility in co-located nodes with a mass flux of 11.9 ± 0.4 kg/h for carbon dioxide and 10.9 ± 0.4 kg/h for methane (release number 9).

Figure D.1 shows the mapped CO_2 concentrations on the flux plane, while Figure D.2 shows the mean gridded values.
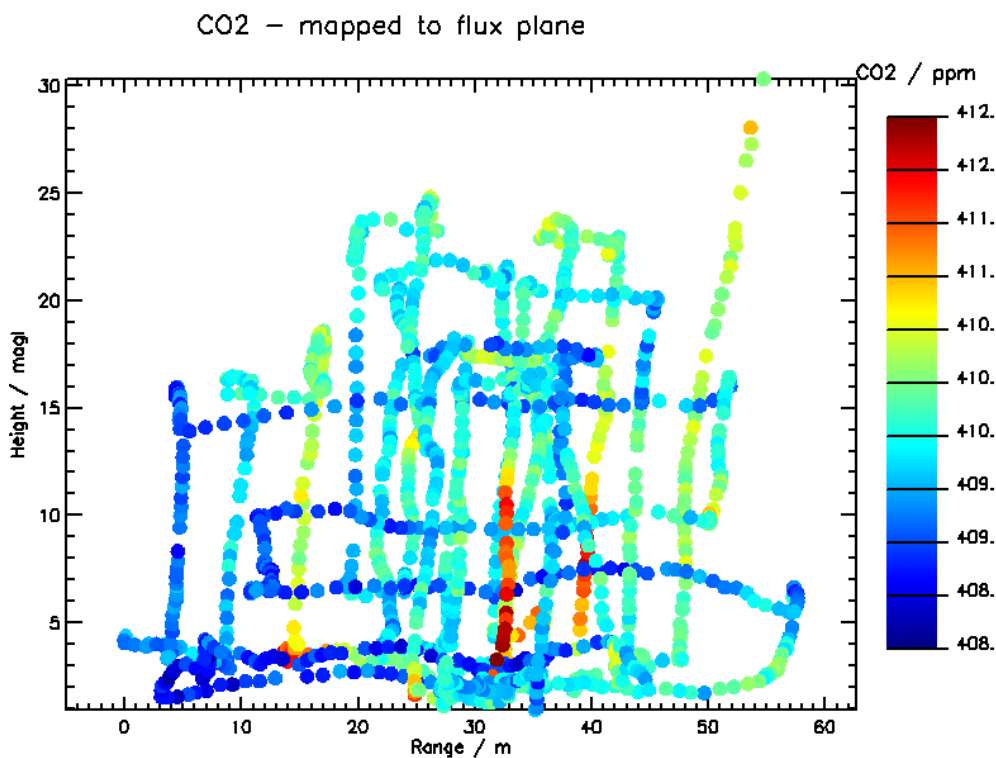
Figure D.1 Carbon dioxide concentrations mapped to UAS flight track and colour-scaled as per legend
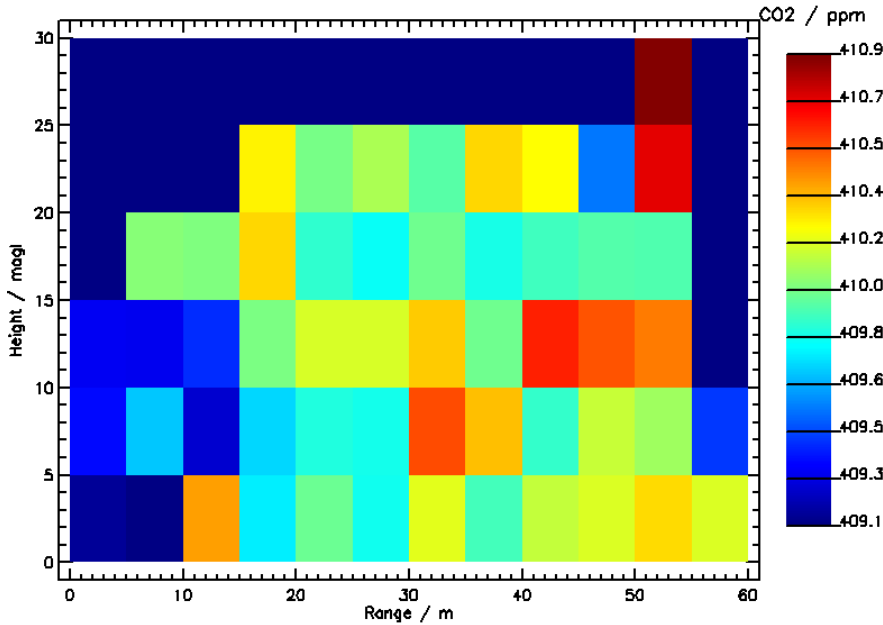
Figure D.2 Carbon dioxide concentrations mapped to UAS flight track and colour-scaled as per legend

Figure D.2 clearly shows the presence of a CO_2 plume in the centre of the flux plane.

The UGGA instrument measures both CO_2 and CH_4. Figure D.3 shows the relationship between measured CO_2 and measured CH_4. We see a very clear correlation, with a mass ratio of around 0.805 between CO_2 andCH_4.
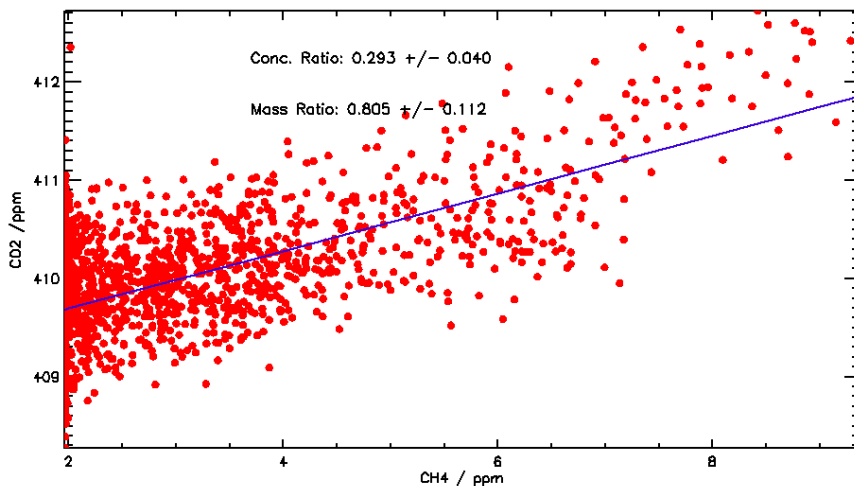
Figure D.3 Mixing line of measured CH_4 and simultaneously measured CO_2 gas concentrations

An example of the data output from our flux analysis software is shown below, indicating the parameters calculated and used in the mass balance flux forward model (Equations 1 and 2)

This example shows that the relative uncertainty on the flux (~20%) is similar to that typical of the CH_4 flux and that wind speed and direction variability dominates the uncertainty budget. The mass flux of CO_2 derived from this flight was 14.18 kg/h (± 3.46 kg/h), compared with the known release rate of 11.9 kg/h. Therefore, there is a positive bias in this example of 2.28 kg/h (19.2%), which is significantly higher than the biases typical for CH_4, although there is still agreement within the stated one standard deviation uncertainty. The larger bias for CO_2 (compared with CH_4) is strongly expected to be due to the problem of correctly establishing a background (upwind) concentration for CO_2, which is known to vary more in the ambient atmosphere due to the large range of CO_2 emission sources. Background CO_2 concentrations were observed to vary by up to 5 ppm (or

1.25% of typical ambient averages) over the timescale of an hour while the UGGA instrument was operated on the ground (when not used for UAS experiments). This compared with analogous background variability of CH_4 of less than 10 ppb (0.5%). This enhanced CO_2 variability makes it more difficult to establish a representative background that can be used in Equation 1, and if a linear trend (drift) in ambient CO_2 were to occur over the timescale of a flight then this would be convolved with the downwind measurements and directly result in a biased flux with the sign of the ambient drift. Such drifts are magnified significantly for CO_2 relative to CH_4 in typical UK land-based environments. One solution to this background problem would be to have a second instrument that measured upwind concentrations continuously and to use those measurements to subtract a fitted temporal spline to downwind sampling, as opposed to subtracting a singularly representative value as formalised in Equation 1. Such a fix would serve to reduce systematic flux bias error but not flux uncertainty, which is a function of randomly varying components identified in Equation 2.

Data example for Flight 2

Flight: 03 Nov 2016, 40640.000- 42320.000 secs since midnight

Max horizontal extent: 57.851039

h diff: 29.369999

Flight orientation = 31.348244 degrees

Mean wind speed for flight: 3.81494 m/s

Mean wind direction for flight: 234.072 degrees

Mean wind perprendicular offset from flight plane: -4.5794604 degrees

Sigma (wind speed): 0.481724 m/s

Sigma (wind direction): 7.51293 degrees

Fitted CO_2/CH_4 mass ratio: 0.805351 ± 0.112153

Fitted CO_2/CH_4 concentration ratio: 0.293520 ± 0.0408757

Mean surface T: 282.043 K

Mean surface P: 1018.09 mb

CH_4 flux plane standard error on mean: 0.387538 g/s

CO_2 flux plane standard error on mean: 0.644809 g/s

CH_4 wind speed error: 0.494035 g/s

CO_2 wind speed error: 0.497383 g/s

CH_4 wind direction error: 0.511550 g/s

CO_2 wind direction error: 0.515017 g/s

CH_4 measurement error: 0.0391243 g/s

CO_2 measurement error: 0.0393895 g/s

Total CH_4 flux (unweighted): 3.91243 ± 0.810846 g/s

Total CO_2 flux (unweighted): 3.93895 ± 0.964346 g/s

Appendix E – Tracer dispersion method

Contents

1. Introduction

The University of Southampton (UoS) and the Technical University of Denmark (DTU) were invited by the Environment Agency to take part in the controlled methane (CH_4) release experiments (not carbon dioxide) being carried out over 3 days from 2 to 4 November 2016 at the Met Office site at Cardington. This would provide two independent, ground-based assessments of CH_4 fluxes to compliment the work being carried out by the University of Manchester (UoM).

The flux rate of the released CH_4 gas was controlled and monitored by the National Physical Laboratory (NPL), and was known only to NPL during the release trials and initial data analysis.

The UoS and DTU released a tracer gas (acetylene, C_2H_2) close to the CH_4 release point(s) and, independently, monitored the CH_4 and C_2H_2 plumes off-site, downwind of the source. C_2H_2 was released at a constant rate from either one or two locations during each CH_4 release.

2. Overview of the tracer dispersion method

The tracer dispersion method (TDM) technique for assessing CH_4 emissions from natural and anthropogenic sources (e.g. landfill or waste water treatment plants) has been under continual development, especially in response to improvements in the portability and range of trace gases that can be analysed by field instruments. Current state-of-the-art TDM tests for determining CH_4 emissions from landfills involve using C_2H_2 as the tracer gas, released on the landfill. Measurements of the tracer gas and CH_4 concentrations are made downwind of the source. The use of an inert tracer such as C_2H_2, N_2O or perfluorocarbon are well described (see Roscioli et al. 2015, Foster-Wittig et al. 2015, Mønster et al. 2014, 2015). The TDM technique relies on the assumption that full mixing between the tracer gas and landfill CH_4 plume has occurred at the monitoring point.

2.1. Theoretical basis

The TDM combines a controlled release of tracer gas from the landfill, with CH_4 and tracer concentration measurements downwind of the landfill using a mobile high-resolution analytical instrument (Börjesson et al. 2009; 2007; Galle et al. 2001; Scheutz et al. 2011). The method has been used successfully since the 1990s, and with new developments in analytical technology it has become a powerful tool for quantifying CH_4 emissions from landfills (Mønster et al. 2014, 2015).

The TDM is based on the assumption that a tracer gas released at a CH_4 emission source will disperse in the atmosphere in the same way as the emitted CH_4. Assuming a defined wind direction, well-mixed air above the landfill (causing the emitted CH_4 and released tracer gas to be fully mixed), and a constant tracer gas release rate, the CH_4 emission rate can be calculated as a function of the ratio of the integrated cross-plume concentration of the emitted CH_4 and the integrated cross-plume concentration of the released tracer gas.

Downwind measurements are typically carried out along public highways around the landfill, with monitoring distances and location varying depending on the wind direction, the degree of dispersion, the accessibility of roads, and possible interference with other CH_4 sources. The location of the tracer gas bottles in relation to the source of the CH_4 is also important, as poorly located tracer gas may result in an off-set between the tracer gas plume and CH_4 plumes. Even if there is no off-set at the start, this may change if the wind direction changes.

The release of tracer gas should be closely controlled to ensure a steady and continuous release. Conservative time windows, at the start and end of the tracer release, are recommended, to ensure that the tracer gas release is at steady state during the measurement period.

The optimal distance for measuring a site's total emissions depends on the size of the emission area, the topography of the site and weather conditions such as wind speed and solar radiation (Mønster et al. 2014). At each plume transect, it is important that the whole plume is measured before turning the vehicle to measure the plume again. This allows for an average background concentration to be subtracted from the measurements, in order to obtain just the landfill's contribution to the plume.

2.2. Data analysis methods

Assuming a defined wind direction, well-mixed air above the landfill (causing the emitted CH_4 and released tracer gas to be fully mixed) and a constant tracer gas release, the CH_4 emission rate can be calculated as a function of the ratio of the integrated cross-plume concentration of the emitted CH_4 and the integrated cross-plume concentration of the released tracer gas, as follows:

$$E_{gas} = Q_{tracer} \cdot \frac{\int_{P_{g1}}^{P_{g2}} C_{gas}\, dx}{\int_{P_{t1}}^{P_{t2}} C_{tracer}\, dx} \cdot \frac{MW_{gas}}{MW_{tracer}} \qquad \text{(Equation E.1)}$$

Where E_{gas} is the CH_4 mass flow rate (kg/h), Q_{tracer} is the release rate of the tracer gas (kg/h), C_{gas} and C_{tracer} denote cross-plume concentrations above the background concentration, P_g and P_t denote the plume for the gas and tracer respectively, MW denotes molecular weight and x corresponds to distance across the plume.

Depending on the duration of the tracer release, a large number of transects (between 10 and 30) may be made through the plumes during each tracer gas release, though not all transects will always be used in CH_4 quantification. A visual screening of each transect is recommended, to check for anomalous data and excess noise, which may be caused by instrument error, changing weather patterns and from interfering CH_4/C_2H_2 sources. Where concentrations are low, close to the background measurement or close to the detection limits of the analyser, it may also be difficult to distinguish the gas plume from the noise in the background data.

The plume transects passing visual screening are individually integrated to calculate the CH_4/C_2H_2 ratio. The CH_4 emission rate can then be calculated using Equation E.1. The CH_4 emission from the landfill is typically given as the average (and a standard deviation) of the emissions measured in each plume transect. If the CH_4 emission is constant in time, the standard deviation will in most cases decrease with an increase in the number of plume transects. For this reason, a large number of transects (> 10-15) are recommended (Mønster et al. 2014).

3. Application of TDM to the Cardington CH_4 release trial

3.1. UoS and DTU instrumentation

3.1.1. UoS system

The instrumentation used in the trials was a Ultraportable CH_4-C_2H_2 analyser (Los Gatos Research) (LGA). This was fitted with an external pump (KNF, N920) to allow a higher through-flow of air than the inbuilt LGA pump. The LGA was connected to a datalogger and output in real-

time allowing the concentration of both CH_4 and C_2H_2 to be monitored. The precision of the measurements was 2 ppb for both gases.

The LGA and pump were placed in the back of a van and connected to an inlet hose, which passed through the top of the nearside door to sample the outside atmosphere. A Garmin 18x-PC GNSS receiver connected to the datalogger was utilised to log the position of the monitoring vehicle. The LGA and GNSS had a synchronised logging rate of 1 Hz.

Whilst using the LGA for these trials, it became apparent that the flow through time was significantly less than was expected from the performance specification of the external pump. Tests carried out using gas standards directly following the Cardington tests, revealed a systematic lag in the detection time (i.e. time from gas entering the sampling tube to first registering a change in concentration above background), the fully mixed time (i.e. time in which the measured gas concentration reaches the input gas concentration), and the subsequent clear-out time (i.e. time from stopping the input gas and concentrations returning to background). The detection lag and peak flow lag were the same for both CH_4 and C_2H_2.

The data presented has been corrected for detection time lag (21 seconds), but not for the fully-mixed or clear-out time. This has the effect of creating asymmetrical profiles, with the leading limb of the plume profile being slightly steeper than the tailing limb. However, since analysis of the method (sections 2.1 and 5.1 of this appendix) predominantly involves the integration of the cross-plume concentration of CH_4 compared to that of C_2H_2, this measurement discrepancy was not expected to significantly affect the analysis.

During an individual profile transect the monitoring vehicle was driven as much as possible at a constant speed. This varied depending on driving conditions and local traffic, but typically varied between 26 and 29 km/h.

3.1.2. DTU system

The analytical platform used by DTU was a vehicle-mounted CH_4/C_2H_2 detector and GNSS system similar to the system described in Mønster et al. (2014, 2015). Measurements were performed with a cavity ring-down spectroscopy, CH_4/C_2H_2 analyser (G2203, Picarro Inc., USA). Atmospheric air was sampled from the roof of the monitoring vehicle and brought to the analyser via an external pump, enabling a fast response time while driving. The atmospheric concentrations of CH_4, C_2H_2 and water were measured with a frequency of 2 Hz and logged together with the GPS position. The precisions of CH_4 and C_2H_2 measurements were 0.48 ppb and 0.40 ppb, respectively.

A GNSS receiver (model R330 Receiver and A43 Antenna, Hemisphere, Canada) was used to log the position of the monitoring vehicle, measured within 0.30 m precision. Driving speed while measuring was as constant as practically possible, and was between 20 and 30 km/hour. A weather station mounted on the vehicle (All-In-One weather sensor, model 102780, Climatronics, USA) measured temperature, atmospheric pressure, wind speed and wind direction, although the site meteorological data was used in the analysis to be consistent with the other monitoring teams.

3.2. CH_4 and C_2H_2 release information

A total of 12 controlled gas release trials were carried out over the course of the experiment, though only five included the release of CH_4 (Releases 8 to 12). Details of the CH_4 release trials and methodology are given in the main report Section 4.2 and in Appendix A. The location of the CH_4 release points is shown in Figure E3.1.

3.2.1. C_2H_2 release system

C_2H_2 was released directly from 16 litre C_2H_2 bottles fitted with a pressure regulator and flow meter. Either one or two C_2H_2 bottles were used in a test at a given time. Where two bottles were used, they were spaced no more than 1 m apart. Bottles were weighed before and after use to determine the mass loss using a platform scale with a reproducibility of 50 g (Measuretek, EHI-B102). The location of the acetylene bottles for each release are shown in Figure E3.1.

'Floating-ball' type flow meters (ShoRate, Brooks Instruments, USA) were used to set the C_2H_2 release rate. Flow was adjusted manually using a pin-valve and was checked regularly to ensure flow was consistent and constant throughout the release.

The average mass flow has been calculated for each test (mass used/time). These are given in Table E3.1. The C_2H_2 purchased (BOC Gases) has a minimum purity of 98%. The platform scale has an error of 0.1%. The calculated mass flow, therefore, has a combined negative error of ~2%. An error of 2% is shown as a negative error bar in the mass flow plots in section 5 of this appendix.

Table E3.1. Details of C_2H_2 release

Release number	No. bottles used	Date and time (GMT)	Time	Release position (latitude, longitude)	Mass-based calculated flux rate (kg/h)
8	2	2/11/16	14:57 to 16:36	-0.42367, 52.10464	1.727
9	1	3/11/16	10:42 to 12:19	-0.42352, 52.10447	0.990
10	2	3/11/16	14:37 to 15:45	-0.42451, 52.10352	2.074
11	2	3/11/16	15:52 to 16:41	-0.42451, 52.10352	2.020
12	2	4/11/16	08:32 to 10:03	-0.42352, 52.10447	1.451

Figure E3.1. CH$_4$ and C$_2$H$_2$ release points within the Met Office field site
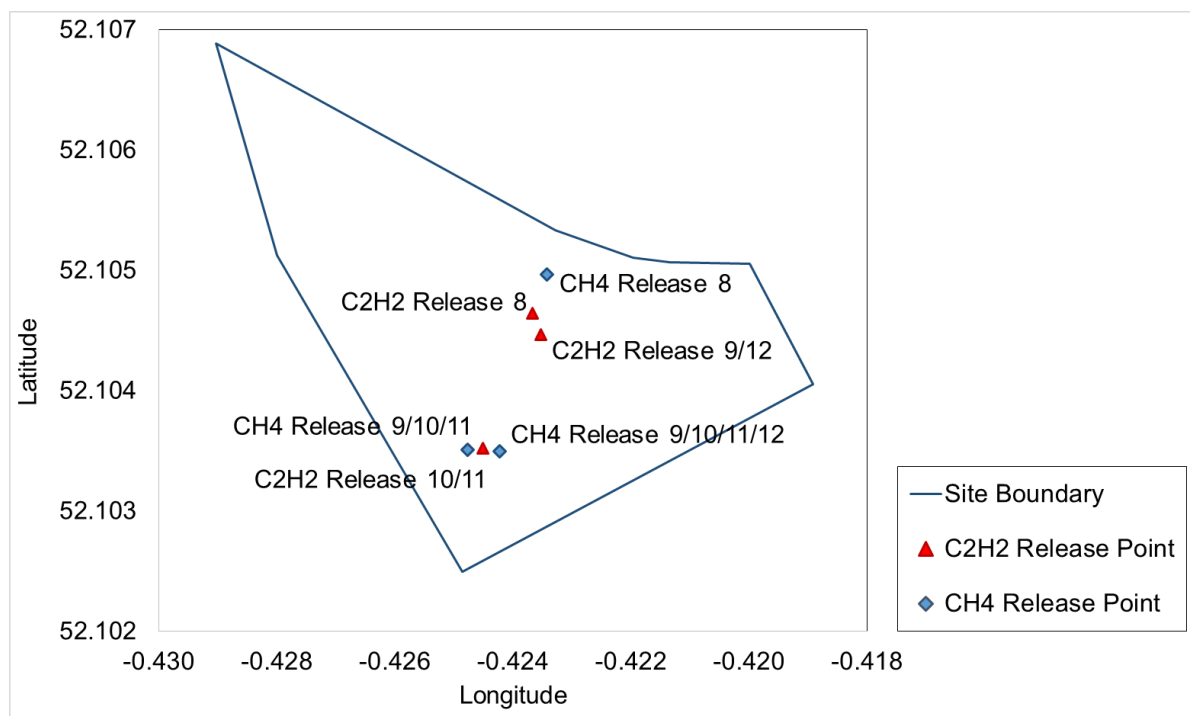
3.3. Background Screening

Several minor and major roads surround the field site (described in section 3 of the main report). No access was available to private land outside of the Met Office field site. Background screening was carried out on 28 October 2016, five days preceding the tracer release experiments. During this time, the wind was from the NW. Screening was to check for any significant sources of CH_4/C_2H_2 in the vicinity of the airfield that might interfere with the experimental results. A number of historic, closed landfill sites are present to the north and west of the airfield. A Google Earth (2017) image showing the location of the sites is given in Figure E3.2. No significant emissions were detected from any of the sites, or at any location along the screening routes (Figure E3.3).

During releases 9 to 12 the wind was from the southwest. A large pile of manure to the northeast of the airfield (shown on Figure E3.2) was noted to emit CH_4. The plume from the manure pile was clearly detectable, often with a higher local CH_4 concentration than the test gas (Figure E3.4). The high CH_4 concentration from the manure pile is most likely due to its close proximity to the road and the measuring vehicle, and not necessarily due to a very high CH_4 emission. Although it was usually possible to distinguish between the two (from the C_2H_2 data), where any overlap occurred, the data was not used in the mass flow calculations.

The location of known licensed and historic landfill sites (orange), Met Office site (yellow) and routes driven for background screening (blue, CH_4; red, C_2H_2) on 28 October 2016 are shown in Figure E3.2. Average wind direction is shown by the arrow. The location of the manure pile is shown by the white pin.

Figure E3.2. Site location (Google Earth 2017)

Figure E3.3. Background CH₄ (blue) and C₂H₂ (red) concentrations measured during pre-test screening on 28 October 2016 (note: no C₂H₂ data was logged before 11:21)
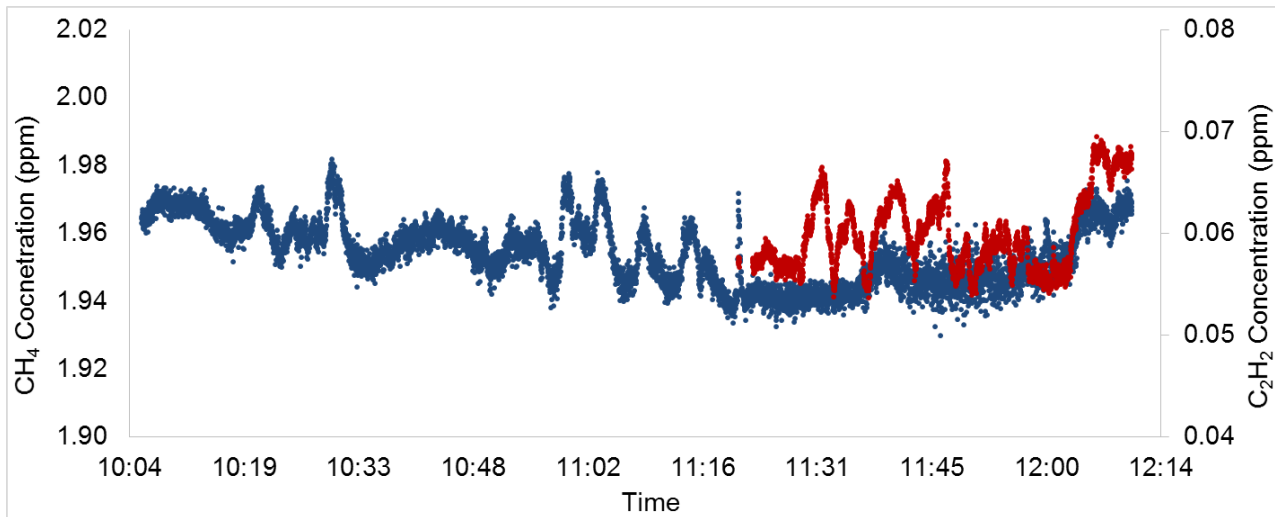
Figure E3.4. Example CH₄ signal from the manure pile close to the signal from test gases (Transect UOS 11.6)
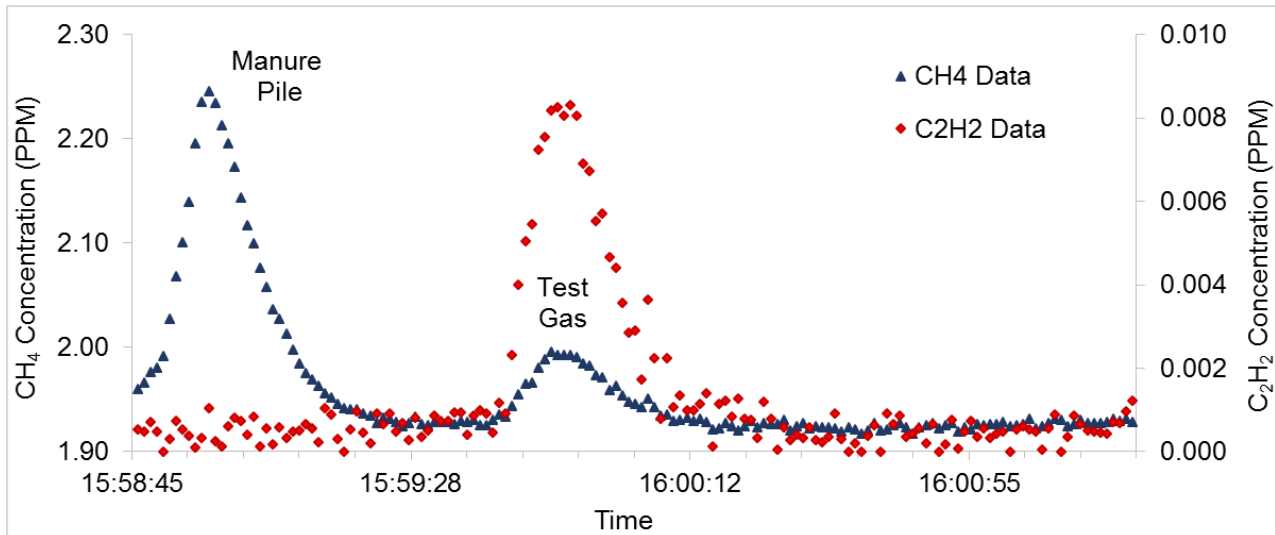
4. Results – raw data

4.1. UoS raw data

Table E4.1. Summary of UoS test data

Release no.	Date	Time	Dominant wind direction*	No. of CH$_4$ release points	No. of C$_2$H$_2$ release points	C$_2$H$_2$ mass flow rate (kg/h)	No. of transects through plume	No of transects used in analysis	Mean distance from source (km)
8	2/11/16	12:57 to 16:36	NW 311 to 320	1	2	1.727	2	2	1.6
9	3/11/16	10:32 to 12:19	SW 229 to 236	2	1	0.990	15	7	1.2
10	3/11/16	14:28 to 15:30	SW 221 to 229	2	2	1.831	5	5	1.2
11	3/11/16	15:35 to 16:40	SW 211 to 232	2	2	1.456	16	6	1.2
12	4/11/16	08:32 to 10:03	SW 229 to 239	1	2	1.451	12	8	1.2 and 3.5

*Cardinal degrees

The wind direction was relatively stable during each release, but differed somewhat on each release day. Monitoring routes were dependent on the wind direction. For Release 8, the wind was from the northwest, ranging between 311 and 320 degrees. The monitoring route had a heading of 40.6 degrees, making the angle between the wind and plume measurement 94 degrees. For Releases 9 to 12, the wind direction was from the southwest ranging between 211 and 239 degrees. The main monitoring route had a dominant heading of 315 degrees, making the angle between the wind and the plume measurements 76 to 104 degrees.

For Release 12, transects UOS 12.3 and UOS 12.6, a more distant monitoring route was also used. This route had a heading of 358 degrees, making the angle between the plume and wind 119 degrees.

Sections 4.1.1 to 4.1.5 of this appendix give details of individual transect data from each release that was then used in the analysis of CH$_4$ flow rates. A Google Earth (2017) image is shown for each release to illustrate the measured location of the plume with respect to the release points. Plume data from a representative transect is shown: CH$_4$ data in blue and C$_2$H$_2$ data in red. The vertical scale of the data histograms have been exaggerated to aid in viewing and are not necessarily scaled relative to each gas' measured concentration. The data has been corrected for the LGA detection delay. Average wind direction is shown by the yellow arrow and the direction of the monitoring vehicle is shown by the green arrow.

Only transects that had good plume matching have been used in the calculation of CH$_4$ fluxes. This was to simplify the analysis of the UoS data as discussed in section 5.2 below. Figures E4.1a and E4.2a show example data from two transects from Release 9. In Figure E4.1a, there is good plume matching (plumes overlie), whereas in Figure E4.2a, there is a significant off-set in the plumes. When the concentration data are regressed (CH$_4$/C$_2$H$_2$), an off-set in the plumes will result in a lower R^2 (how well the data lie along the fitted regression) than well-matched plumes. This is demonstrated in Figure E4.1b and E4.2b. Possible reasons for the plume off-set are discussed in section 5 below, but may be due to a change in the wind direction during the course of the experiment.

Transects may also have been rejected due to noisy data (which will also result in a low R^2) in which it is difficult to discern the edges of the plume and/or determine a representative background concentration.

Figure E4.1 Example of good plume matching. Transect UOS 9.7
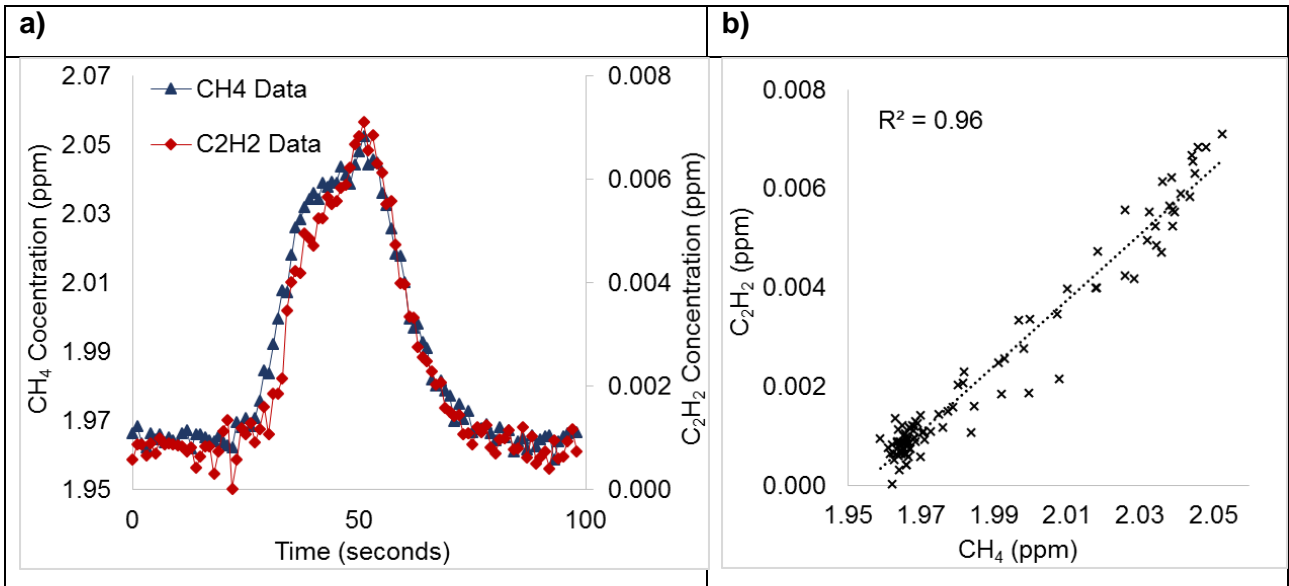
Figure E4.2 Example of off-set plumes. Data rejected from further analysis. Transect UOS 9.12
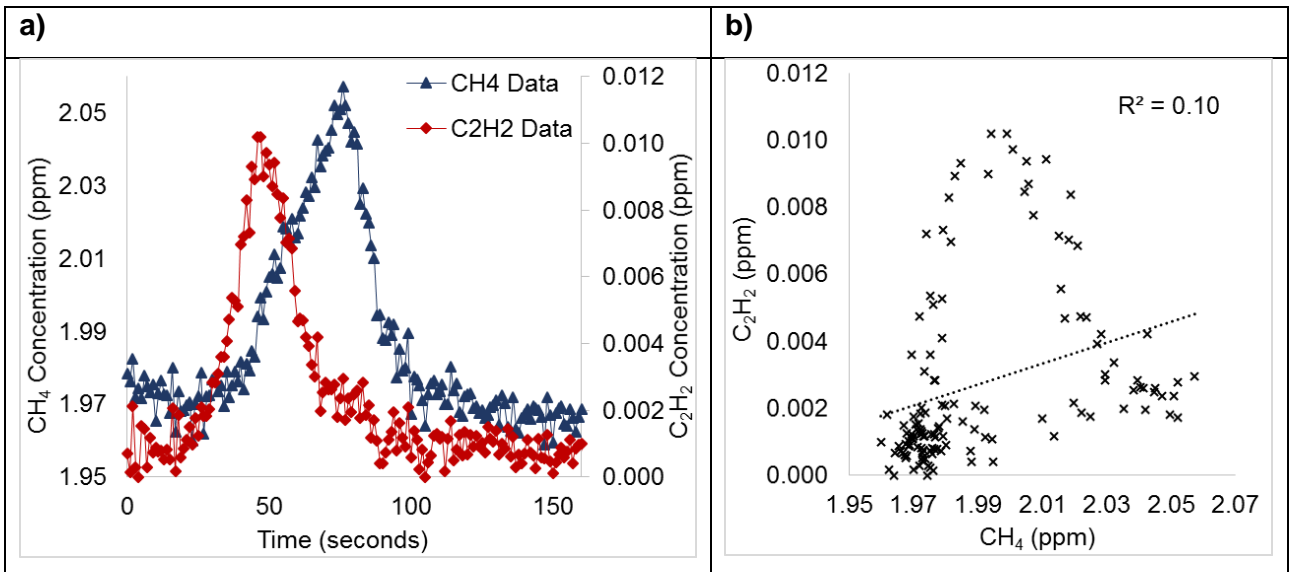
4.1.1. UoS transect data from Release 8

Table E4.2 Summary of Release 8 results

Transect no.	Start of transect (HH:MM:SS)	Wind direction (degrees)	Mean distance from source (km)	Average CH_4 background (ppm)	Average C_2H_2 background (ppm)	R^2
UOS 8.1	16:07:40	315	1.6	1.956	0.0034	0.94
UOS 8.2	16:12:24	315	1.6	1.951	0.0020	0.97

Figure E4.3 Release 8 gas release points, wind direction and monitoring route. Transect UOS 8.1 (Google Earth 2017)

4.1.2. UoS transect data from Release 9

Table E4.3 Summary of Release 9 results

Transect no.	Start of transect (HH:MM:SS)	Wind direction (degrees)	Mean distance from source (km)	Average CH_4 background (ppm)	Average C_2H_2 background (ppm)	R^2
UOS 9.6	11:44:55	229	1.2	1.963	0.0007	0.86
UOS 9.7	11:48:14	230	1.2	1.965	0.0008	0.96
UOS 9.9	11:54:53	232	1.2	1.967	0.0008	0.76
UOS 9.10	11:58:37	233	1.2	1.971	0.0009	0.68
UOS 9.11	12:02:24	233	1.2	1.969	0.0009	0.73
UOS 9.13	12:10:04	236	1.2	1.968	0.0008	0.72
UOS 9.15	12:15:57	236	1.2	1.967	0.0009	0.81

Figure E4.4 Release 9 gas release points, wind direction and monitoring route. Transect UOS 9.6 (Google Earth 2017)

4.1.3. UoS transect data from Release 10

Table E4.4 Summary of Release 10 results

Transect no.	Start of transect (HH:MM:SS)	Wind direction (degrees)	Mean distance from source (km)	Average CH_4 background (ppm)	Average C_2H_2 background (ppm)	R^2
UOS 10.1	15:11:46	221	1.2	1.955	0.0008	0.77
UOS 10.2	15:15:52	221	1.2	1.950	0.0008	0.97
UOS 10.3	15:19:27	224	1.2	1.947	0.0010	0.95
UOS 10.4	15:22:47	224	1.2	1.943	0.0010	0.96
UOS 10.5	15:26:19	229	1.2	1.941	0.0010	0.98

Figure E4.5 Release 10 gas release points, wind direction and monitoring route. Transect UOS 10.4 (Google Earth 2017)
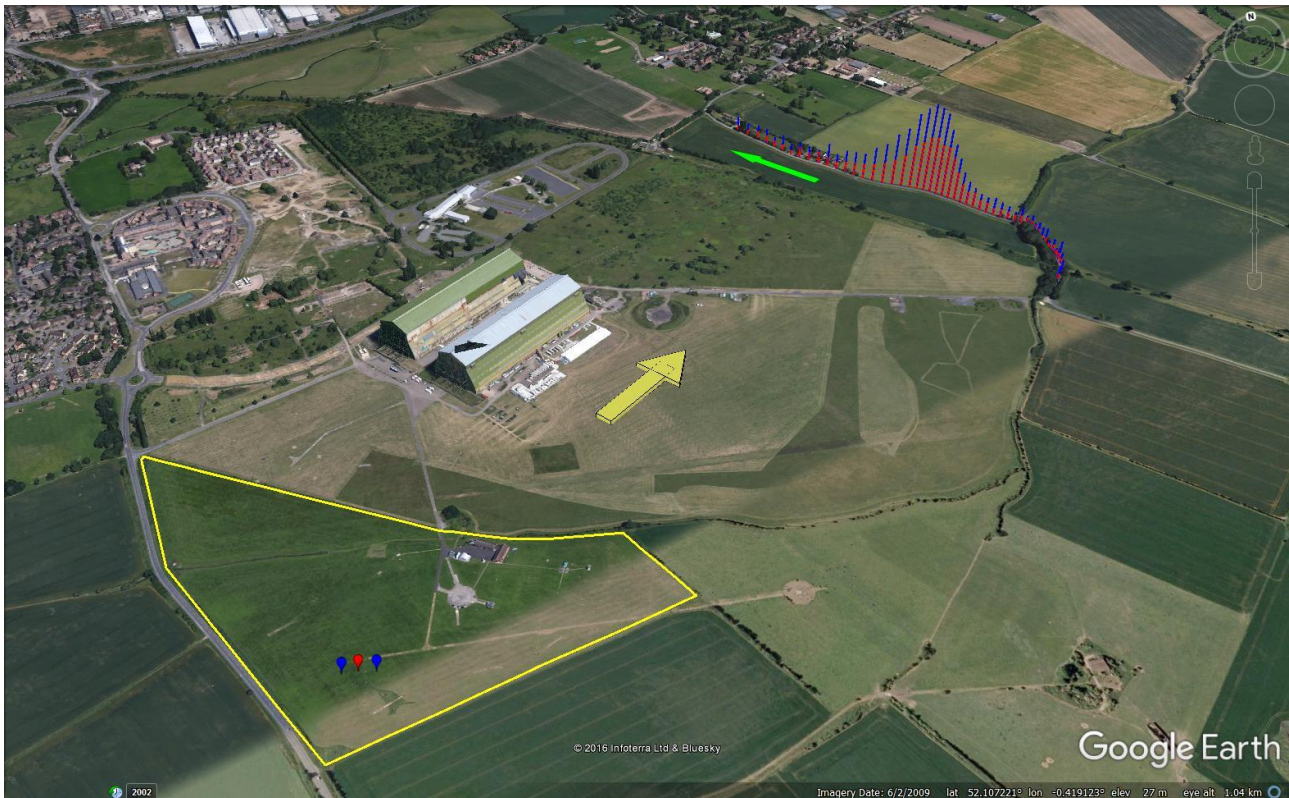
4.1.4. UoS transect data from Release 11

Table E4.5 Summary of Release 11 results

Transect no.	Start of transect (HH:MM:SS)	Wind direction (degrees)	Mean distance from source (km)	Average CH_4 background (ppm)	Average C_2H_2 background (ppm)	R^2
UOS 11.1	15:40:50	232	1.2	1.927	0.0007	0.74
UOS 11.2	15:44:53	231	1.2	1.926	0.0006	0.74
UOS 11.3	15:47:44	231	1.2	1.925	0.0007	0.95
UOS 11.6	15:59:25	223	1.2	1.926	0.0006	0.98
UOS 11.7	16:03:02	219	1.2	1.925	0.0006	0.98
UOS 11.8	16:06:08	216	1.2	1.928	0.0007	0.97
UOS 11.9	16:14:10	214	1.2	1.932	0.0007	0.96

Figure E4.6 Release 11 gas release points, wind direction and monitoring route. Transect UOS 11.7 (Google Earth 2017)

4.1.5. UoS transect data from Release 12

Table E4.6 Summary of Release 12 results

Transect no.	Start of transect (HH:MM:SS)	Wind direction (degrees)	Mean distance from source (km)	Average CH$_4$ background (ppm)	Average C$_2$H$_2$ background (ppm)	R^2
UOS 12.1	08:57:38	229	1.25	1.993	0.0000	0.86
UOS 12.2	09:04:35	233	1.25	1.986	0.0001	0.93
UOS 12.3	09:12:55	233	3.56	1.995	0.0002	0.72
UOS 12.6	09:22:34	233	3.56	1.965	0.0002	0.61
UOS 12.7	09:35:31	237	1.25	1.952	0.0007	0.87
UOS 12.8	09:37:23	237	1.25	1.950	0.0008	0.58
UOS 12.9	09:43:07	237	1.25	1.951	0.0006	0.66
UOS 12.10	09:45:38	237	1.25	1.949	0.0006	0.94

Figure E4.7 Release 12 gas release points, wind direction and monitoring route. Transects UOS 12.2 (near) and 12.3 (far) (Google Earth 2017)

4.2. DTU raw data

Table E4.7 Summary of DTU test data

Release no.	Date	Time	Dominant wind direction	No. of CH_4 release points	No. of C_2H_2 release points	Tracer mass flow rate (kg/h)	No. of transects through plume	No. of transects used in analysis	Approx. distance from source (km)
8	2/11/16	14:57 to 16:35	NW 311 to 320	1	2	1.727	28	20	1.6
9	3/11/16	10:42 to 12:19	SW 229 to 236	2	1	0.990	33	27	1.2
10	3/11/16	14:37 to 15:45	SW 221 to 229	2	2	1.831	14	12	1.2
11	3/11/16	15:52 to 16:41	SW 211 to 232	2	2	1.456	7	6	1.2

The DTU measurements were performed using the same downwind measurement locations as UoS, with the exception of Release 12, where only UoS performed measurements. Wind directions and measurement routes were, therefore, similar to those described in Section 4.1 of this appendix. Some transects were discarded from further analysis, largely based on the amount of noise in the data, or where the transects were measured after the release of CH_4 had finished.

Sections 4.2.1 to 4.2.4 below, give a summary of the transects used in the analysis of CH_4 flow rates. The data includes the background (BG) concentrations deducted from raw data. For each transect, the R^2 has been calculated from the linear regression of the CH_4 and C_2H_2 data (measured concentrations including background).

For each of the four CH_4 releases, an example of a transect mapped in Google Earth (2017) is given The image shows the location of the measured downwind plumes, location of CH_4 and C_2H_2 gas release (red and yellow triangles, respectively) and the dominant wind direction. The red and yellow lines signify, respectively, measured CH_4 and C_2H_2 concentrations above background level.

During Release 9, 10 and 11, the measurement frequency of the Picarro CH_4/C_2H_2 analyser was reduced from 2 Hz to approximately 0.3 Hz. The cause of this deviance from the instruments' specifications was unknown. The reduced measurement frequency did, however, not appear to influence the precision of the method significantly, since the difference between actual and measured CH_4 emissions was not higher when measuring while the measurement frequency was reduced. The reduced measurement frequency may be the cause of lower R^2 values for Release 9, 10 and 11 compared to Release 8.

4.2.1. DTU transect data from Release 8

Table E4.8 Summary of DTU Release 8 results

Transect no.	Start time	Average CH₄ BG (ppm)	Average C₂H₂ BG (ppm)	R^2	Transect no.	Start time	Average CH₄ BG (ppm)	Average C₂H₂ BG (ppm)	R^2
DTU 8.2	15:22:29	1.956	0.0005	0.86	DTU 8.16	16:06:00	1.965	0.0005	0.84
DTU 8.3	15:26:18	1.956	0.0003	0.76	DTU 8.17	16:08:51	1.957	0.0004	0.72
DTU 8.4	15:32:51	1.956	0.0003	0.96	DTU 8.18	16:12:19	1.965	0.0004	0.88
DTU 8.7	15:40:33	1.956	0.0004	0.84	DTU 8.19	16:15:42	1.960	0.0004	0.87
DTU 8.8	15:42:37	1.956	0.0004	0.90	DTU 8.20	16:17:50	1.965	0.0006	0.97
DTU 8.9	15:44:57	1.956	0.0004	0.89	DTU 8.21	16:20:48	1.960	0.0005	0.92
DTU 8.10	15:47:58	1.956	0.0003	0.92	DTU 8.22	16:23:11	1.960	0.0005	0.97
DTU 8.11	15:51:24	1.956	0.0004	0.75	DTU 8.23	16:26:01	1.960	0.0005	0.98
DTU 8.12	15:53:46	1.957	0.0004	0.68	DTU 8.24	16:29:19	1.960	0.0007	0.96
DTU 8.13	15:57:34	1.957	0.0003	0.77	DTU 8.25	16:32:59	1.960	0.0005	0.97

**Figure E4.8 Release 8 gas release points, wind direction and monitoring route. Transect DTU 8.25 (Google Earth 2017)**

4.2.2. DTU transect data from Release 9

Table E4.9 Summary of Release 9 results

Transect no.	Start time	Average CH₄ BG (ppm)	Average C₂H₂ BG (ppm)	R²	Transect no.	Start time	Average CH₄ BG (ppm)	Average C₂H₂ BG (ppm)	R²
DTU 9.2	10:42:09	1.963	0.0012	0.15	DTU 9.17	11:31:35	1.955	0.0012	0.79
DTU 9.3	10:45:15	1.966	0.0013	0.58	DTU 9.19	11:37:26	1.954	0.0011	0.29
DTU 9.4	10:48:31	1.964	0.0013	0.61	DTU 9.20	11:40:55	1.954	0.0011	0.26
DTU 9.5	10:51:39	1.968	0.0012	0.84	DTU 9.21	11:44:12	1.954	0.0011	0.59
DTU 9.6	10:54:47	1.966	0.0012	0.63	DTU 9.22	11:47:20	1.954	0.0012	0.71
DTU 9.7	10:59:47	1.962	0.0012	0.75	DTU 9.23	11:50:36	1.957	0.0011	0.46
DTU 9.8	11:02:57	1.963	0.0012	0.52	DTU 9.24	11:53:41	1.959	0.0011	0.66
DTU 9.9	11:06:01	1.961	0.0012	0.65	DTU 9.25	11:57:08	1.959	0.0011	0.34
DTU 9.10	11:09:00	1.962	0.0012	0.79	DTU 9.27	12:03:20	1.964	0.0012	0.34
DTU 9.11	11:12:05	1.961	0.0011	0.70	DTU 9.28	12:06:39	1.963	0.0011	0.04
DTU 9.13	11:18:23	1.961	0.0012	0.56	DTU 9.29	12:09:49	1.962	0.0011	0.08
DTU 9.14	11:21:15	1.962	0.0012	0.50	DTU 9.30	12:12:58	1.963	0.0011	0.47
DTU 9.15	11:24:35	1.955	0.0012	0.73	DTU 9.31	12:15:57	1.966	0.0011	0.37
DTU 9.16	11:28:08	1.958	0.0012	0.49					

Figure E4.9 Release 9 gas release points, wind direction and monitoring route. Transect DTU 9.7 (Google Earth 2017)
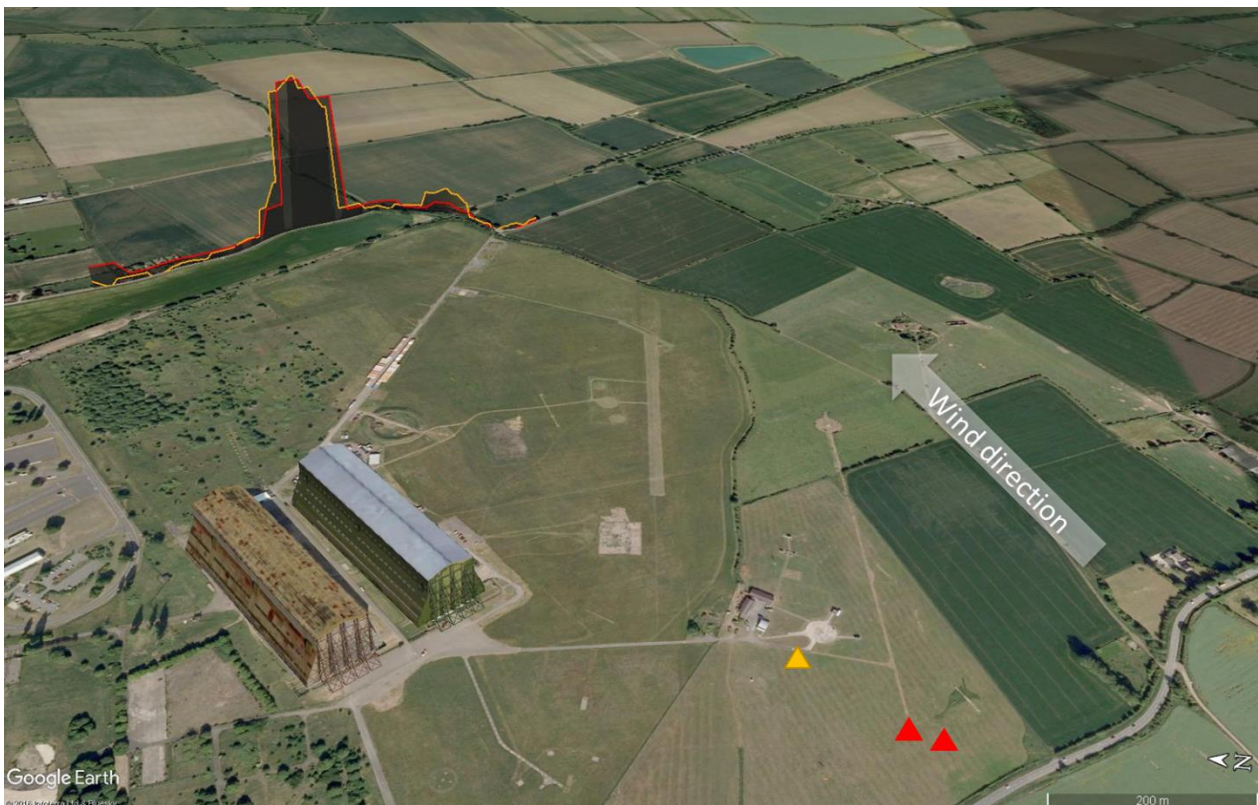
4.2.3. DTU transect data from Release 10

Table E4.10 Summary of Release 10 results

Transect no.	Start time	Average CH_4 BG (ppm)	Average C_2H_2 BG (ppm)	R^2
DTU 10.1	14:48:34	1.950	0.0055	0.79
DTU 10.2	14:52:03	1.950	0.0060	0.30
DTU 10.3	14:54:47	1.948	0.0075	0.67
DTU 10.4	14:58:27	1.948	0.0085	0.82
DTU 10.5	15:01:02	1.949	0.0065	0.71
DTU 10.6	15:05:16	1.948	0.0055	0.74
DTU 10.7	15:07:48	1.948	0.0050	0.72
DTU 10.8	15:12:02	1.947	0.0050	0.64
DTU 10.9	15:14:36	1.947	0.0060	0.68
DTU 10.10	15:18:51	1.947	0.0050	0.56
DTU 10.11	15:25:35	1.943	0.0050	0.71
DTU 10.12	15:28:28	1.945	0.0042	0.72

Figure E4.10 Release 10 gas release points, wind direction and monitoring route. Transect DTU 10.6 (Google Earth 2017)

4.2.4. DTU transect data from Release 11

Table E4.11 Summary of Release 11 results

Transect no.	Start time	Average CH_4 BG (ppm)	Average C_2H_2 BG (ppm)	R^2
DTU 11.1	16:01:44	1.942	0.0004	0.72
DTU 11.2	16:05:43	1.942	0.0004	0.62
DTU 11.3	16:07:52	1.943	0.0004	0.76
DTU 11.4	16:14:46	1.946	0.0003	0.65
DTU 11.5	16:17:01	1.949	0.0008	0.79
DTU 11.6	16:21:08	1.950	0.0008	0.68

Figure E4.11 Release 11 gas release points, wind direction and monitoring route. Transect DTU 11.3 (Google Earth 2017)

5. Analysis and results

5.1. Data processing

For each monitoring transect, the average background concentration was subtracted. This varied between transects, and was calculated by taking the average of the background data measured either side of the plume (Figure E5.1). The background values used are given in Tables E4.2 to E4.11. For the UoS data only, due to the slow flow-through time of the analyser, in some transects high CH_4 concentrations from the manure pile had not fully cleared the analyser before the monitoring vehicle entered the plume. In these instances, background concentrations were determined from the data on the far side of the plume away from the manure pile. This is demonstrated in Figure E5.2.

Figure E5.1 Average background concentrations shown either side of the CH_4 and C_2H_2 plumes. Release 10, Transect UOS 10.4
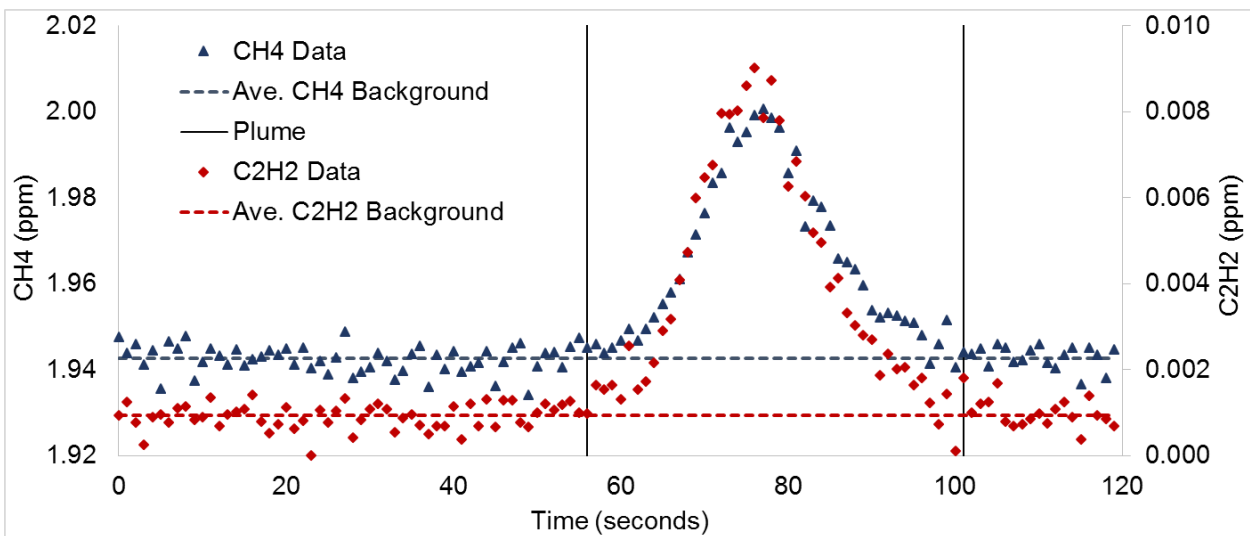
Figure E5.2 Residual CH_4 above background from manure pile, Release 12, Transect UOS 12.7
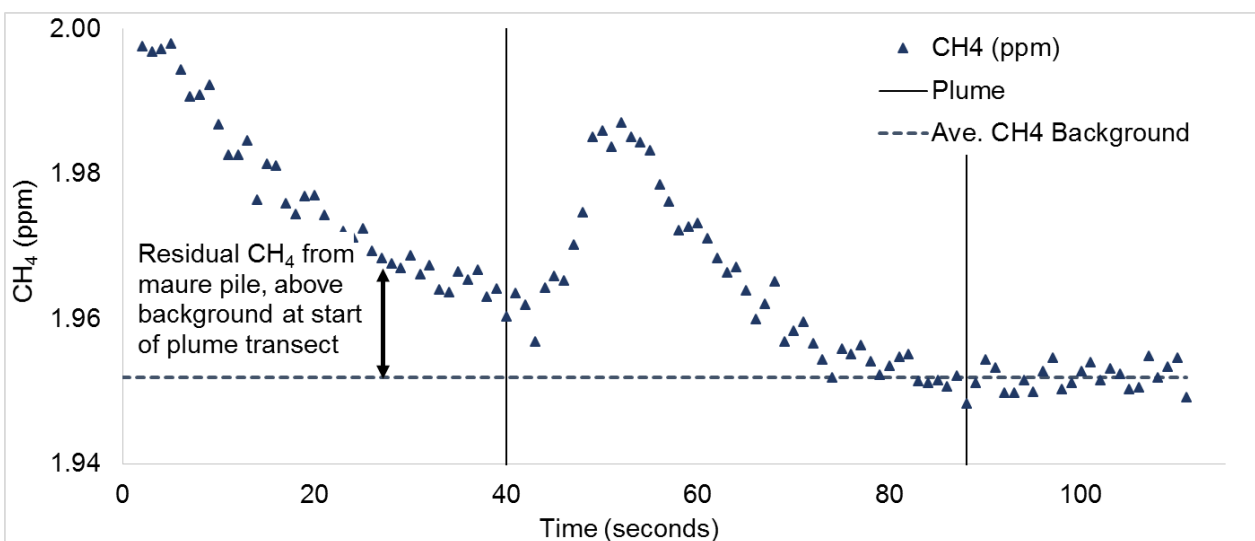
5.2. Mass Flux Calculation

CH_4 mass flux was measured for each of the plume transects given in section 4 of this appendix. This was a blind test, as described in the main report (section 4.1), in that the CH_4 fluxes were unknown to both UoS and the DTU at the time of the analysis.

UoS data were analysed using a simplified version of the mass flux calculation given in Equation E1. In the simplified version, there is an assumption that the integral P_t is equal to P_g. (i.e. that both plumes overlap and have the same start and end-point). This assumption is not valid where the plumes are significantly off-set relative to each other, where the topographical extent of the plumes differs, or where the plume is not perpendicular to the wind.

DTU integrated the CH_4 and C_2H_2 plumes individually ($P_t \neq P_g$), and, therefore, did not reject off-set plumes.

C_2H_2 and CH_4 mass flow are assumed to be constant for the duration of each release. C_2H_2 mass flow is based on mass loss of the C_2H_2 bottles and an assumption of 100% purity. This gives a maximum potential flux.

5.3. Results

Measured CH_4 fluxes for each transect, UoS and DTU data, are given in Tables E5.1 to E5.5. Figures E5.3 to E5.7 show the measured fluxes from each transect plotted with the controlled CH_4 release flux. The average measured fluxes for both the UoS and DTU data are shown. To account for the potentially lower purity of the C_2H_2 gas, a lower error bound (98% purity) has also been plotted.

5.3.1. Results from Release 8

Table E5.1 Results from Release 8

UoS Data

Transect no.	Start time	End time	Measured CH$_4$ mass flow (kg/h)
UOS 8.1	16:07:40	16:11:00	10.76
UOS 8.2	16:12:24	16:14:47	10.12
Average			10.44
SD			0.46

DTU Data

Transect no.	Start time	End time	Measured CH$_4$ mass flow (kg/h)
DTU 8.2	15:22:29	15:24:56	10.75
DTU 8.3	15:26:18	15:28:04	14.26
DTU 8.4	15:32:51	15:34:36	9.88
DTU 8.7	15:40:33	15:42:02	13.04
DTU 8.8	15:42:37	15:44:14	14.59
DTU 8.9	15:44:57	15:47:13	10.68
DTU 8.10	15:47:58	15:49:27	8.08
DTU 8.11	15:51:24	15:52:34	9.34
DTU 8.12	15:53:46	15:55:20	7.77
DTU 8.13	15:57:34	15:59:08	7.79
DTU 8.16	16:06:00	16:07:23	11.69
DTU 8.17	16:08:51	16:10:41	10.03
DTU 8.18	16:12:19	16:14:22	8.47
DTU 8.19	16:15:42	16:17:09	9.94
DTU 8.20	16:17:50	16:19:18	10.37
DTU 8.21	16:20:48	16:22:25	9.76
DTU 8.22	16:23:11	16:24:37	9.11
DTU 8.23	16:26:01	16:28:04	8.13
DTU 8.24	16:29:19	16:31:06	6.97
DTU 8.25	16:32:59	16:35:10	6.60
Average			9.86
SD			2.22

Figure E5.3 Results from Release 8

5.3.2. Results from Release 9

Table E5.2. Results from Release 9

UoS Data

Transect no.	Start time	End time	Measured CH$_4$ mass flow (kg/h)
UOS 9.6	11:44:55	11:46:43	8.36
UOS 9.7	11:48:14	11:49:52	9.41
UOS 9.9	11:54:53	11:56:55	7.32
UOS 9.10	11:58:37	12:00:17	18.33
UOS 9.11	12:02:24	12:04:58	12.89
UOS 9.13	12:10:04	12:12:14	16.30
UOS 9.15	12:15:57	12:19:17	10.52
Average			**11.88**
SD			**4.15**

DTU Data

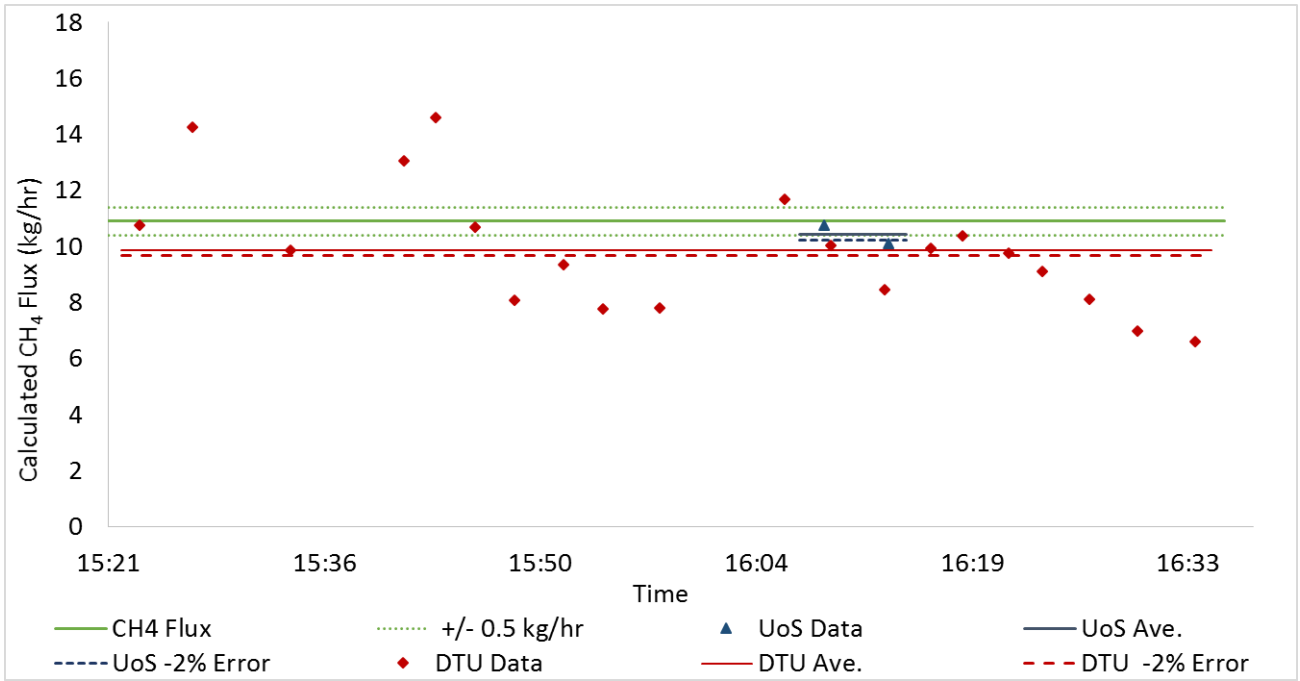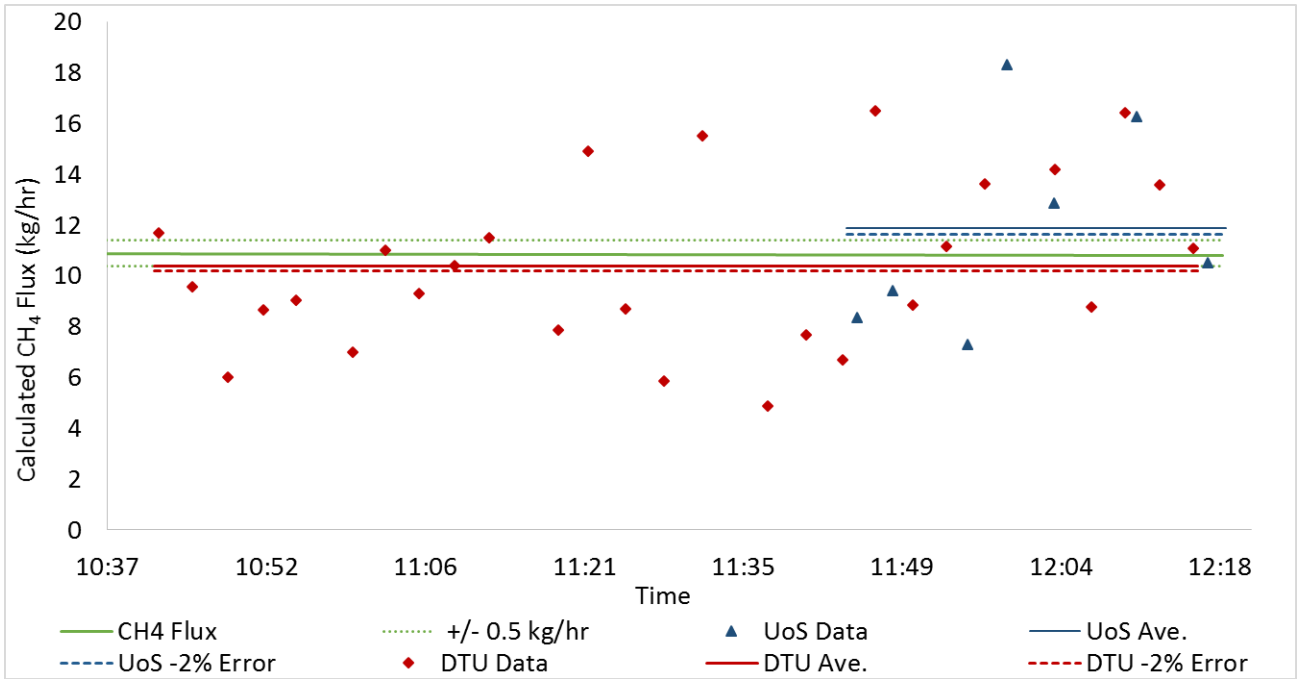| Transect no.	Start time	End Ttme	Measured CH$_4$ mass flow (kg/h)
DTU 9.2	10:42:09	10:42:53	11.70
DTU 9.3	10:45:15	10:45:56	9.58
DTU 9.4	10:48:31	10:49:06	6.02
DTU 9.5	10:51:39	10:52:28	8.67
DTU 9.6	10:54:47	10:55:17	9.03
DTU 9.7	10:59:47	11:00:29	6.99
DTU 9.8	11:02:57	11:03:17	11.00
DTU 9.9	11:06:01	11:06:21	9.32
DTU 9.10	11:09:00	11:09:46	10.40
DTU 9.11	11:12:05	11:12:56	11.52
DTU 9.13	11:18:23	11:19:06	7.89
DTU 9.14	11:21:15	11:21:42	14.93
DTU 9.15	11:24:35	11:25:09	8.70
DTU 9.16	11:28:08	11:28:34	5.85
DTU 9.17	11:31:35	11:32:05	15.53
DTU 9.19	11:37:26	11:38:08	4.89
DTU 9.20	11:40:55	11:41:36	7.69
DTU 9.21	11:44:12	11:44:51	6.70
DTU 9.22	11:47:20	11:47:44	16.50
DTU 9.23	11:50:36	11:51:14	8.84
DTU 9.24	11:53:41	11:54:10	11.15
DTU 9.25	11:57:08	11:57:45	13.62
DTU 9.27	12:03:20	12:04:13	14.19
DTU 9.28	12:06:39	12:07:32	8.77
DTU 9.29	12:09:49	12:10:28	16.45
DTU 9.30	12:12:58	12:13:39	13.61
DTU 9.31	12:15:57	12:16:45	11.10
Average			**10.39**
SD			**3.30**

Figure E5.4 Results from Release 9

5.3.3. Results from Release 10

Table E5.3 Results from Release 10

UoS Data

Transect no.	Start time	End time	Measured CH$_4$ mass flow (kg/h)
UOS 10.1	15:11:46	15:14:11	11.95
UOS 10.2	15:15:53	15:17:32	11.67
UOS 10.3	15:19:28	15:20:32	10.92
UOS 10.4	15:22:48	15:24:46	9.46
UOS 10.5	15:26:20	15:27:49	9.19
Average			**10.64**
SD			**1.258**

DTU Data

Transect no.	Start time	End time	Measured CH$_4$ mass flow (kg/h)
DTU 10.1	14:48:34	14:48:59	10.83
DTU 10.2	14:52:03	14:52:29	8.84
DTU 10.3	14:54:47	14:55:07	12.43
DTU 10.4	14:58:27	14:59:03	11.32
DTU 10.5	15:01:02	15:01:38	15.03
DTU 10.6	15:05:16	15:05:53	12.01
DTU 10.7	15:07:48	15:08:13	15.63
DTU 10.8	15:12:02	15:12:36	10.40
DTU 10.9	15:14:36	15:15:11	11.18
DTU 10.10	15:18:51	15:19:24	7.35
DTU 10.11	15:25:35	15:26:00	6.68
DTU 10.12	15:28:28	15:28:51	12.95
Average			**11.22**
SD			**2.72**

Figure E5.5 Results from Release 10
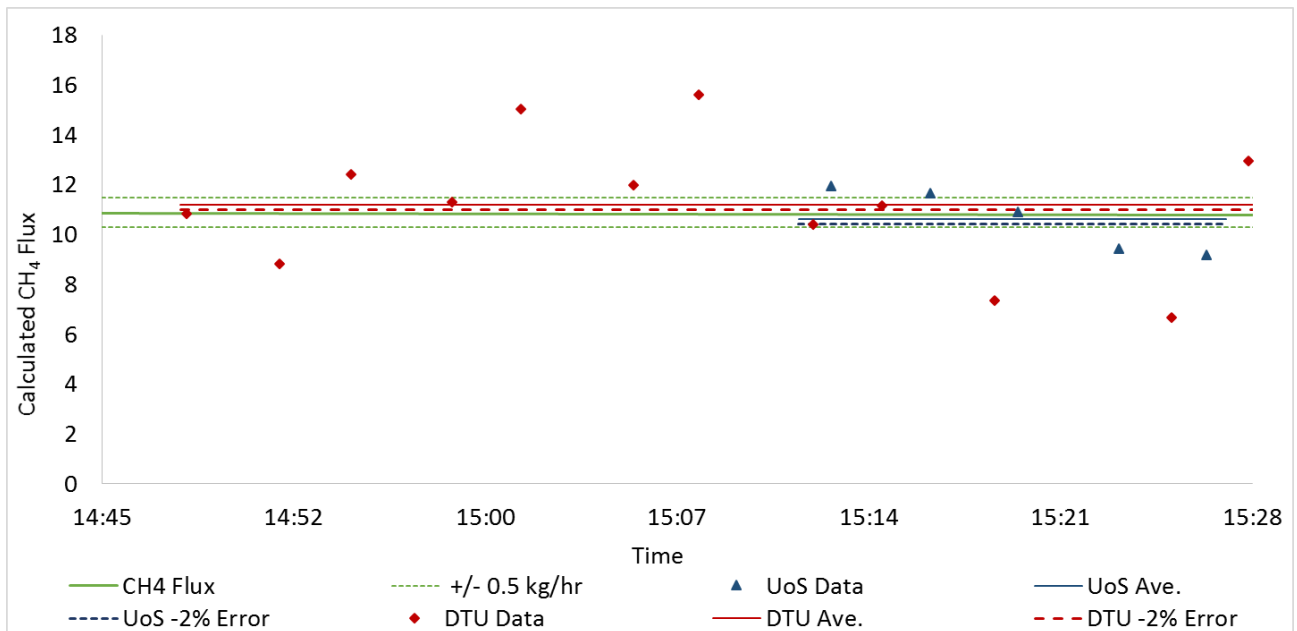
5.3.4. Results from Release 11

Table E5.4 Results from Release 11

UoS Data

Transect no.	Start time	End time	Measured CH$_4$ mass flow (kg/h)
UOS 11.1	15:40:50	15:43:19	5.41
UOS 11.2	15:44:53	15:46:58	6.22
UOS 11.3	15:47:44	15:50:02	5.79
UOS 11.7	16:03:02	16:04:44	5.58
UOS 11.8	16:06:08	16:07:28	4.21
UOS 11.9	16:14:10	16:16:10	5.02
Average			5.37
SD			0.70

DTU Data

Transect no.	Start time	End time	Measured CH$_4$ mass flow (kg/h)
DTU 11.1	16:01:44	16:02:11	4.27
DTU 11.2	16:05:43	16:06:05	4.79
DTU 11.3	16:07:52	16:08:16	4.32
DTU 11.4	16:14:46	16:15:17	4.20
DTU 11.5	16:17:01	16:17:22	4.08
DTU 11.6	16:21:08	16:21:32	4.41
Average			4.34
SD			0.25

Figure E5.6 Results from Release 11
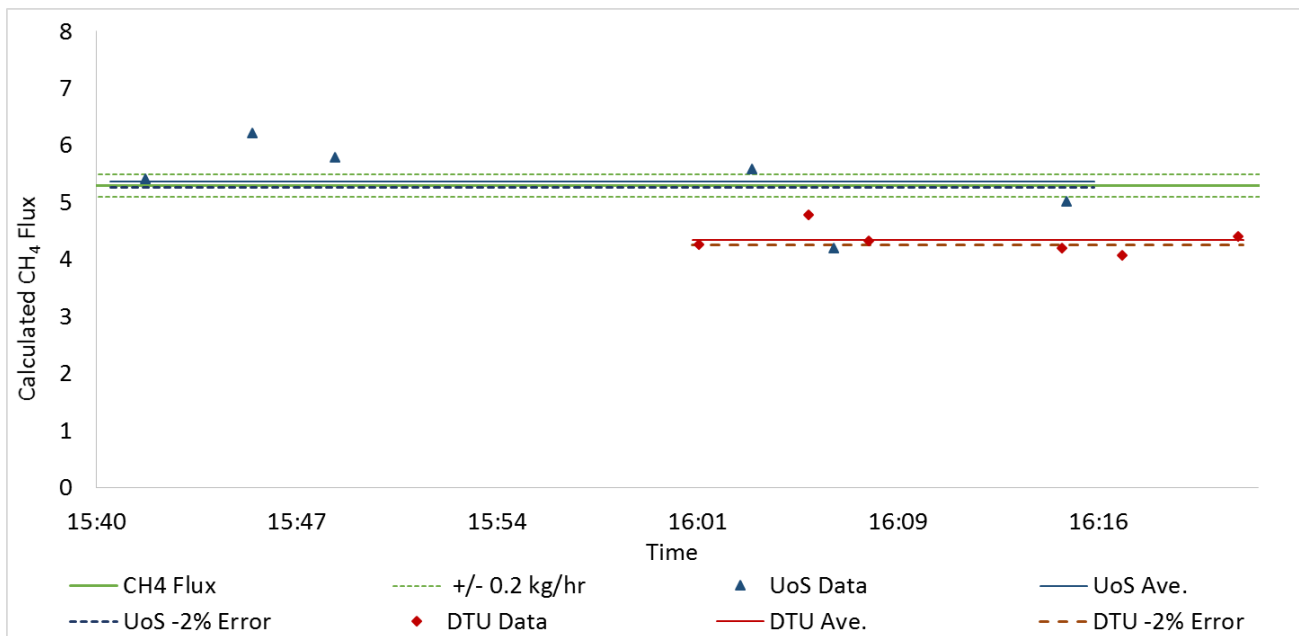
## 5.3.5. Results from Release 12

Table E5.5 Results from Release 12 (only UoS measured Release 12)

UoS Data

Transect no.	Start time	End time	Measured CH_4 mass flow (kg/h)
UOS 12.1	08:57:38	09:01:14	12.34
UOS 12.2	09:04:35	09:10:25	7.25
UOS 12.3	09:12:55	09:15:25	6.32
UOS 12.6	09:22:34	09:27:50	13.83
UOS 12.7	09:35:31	09:37:22	14.95
UOS 12.8	09:37:23	09:40:46	16.86
UOS 12.9	09:43:07	09:45:04	11.31
UOS 12.10	09:45:05	09:48:25	13.04
Average			11.99
SD			3.63

Figure E5.7 Results from Release 12
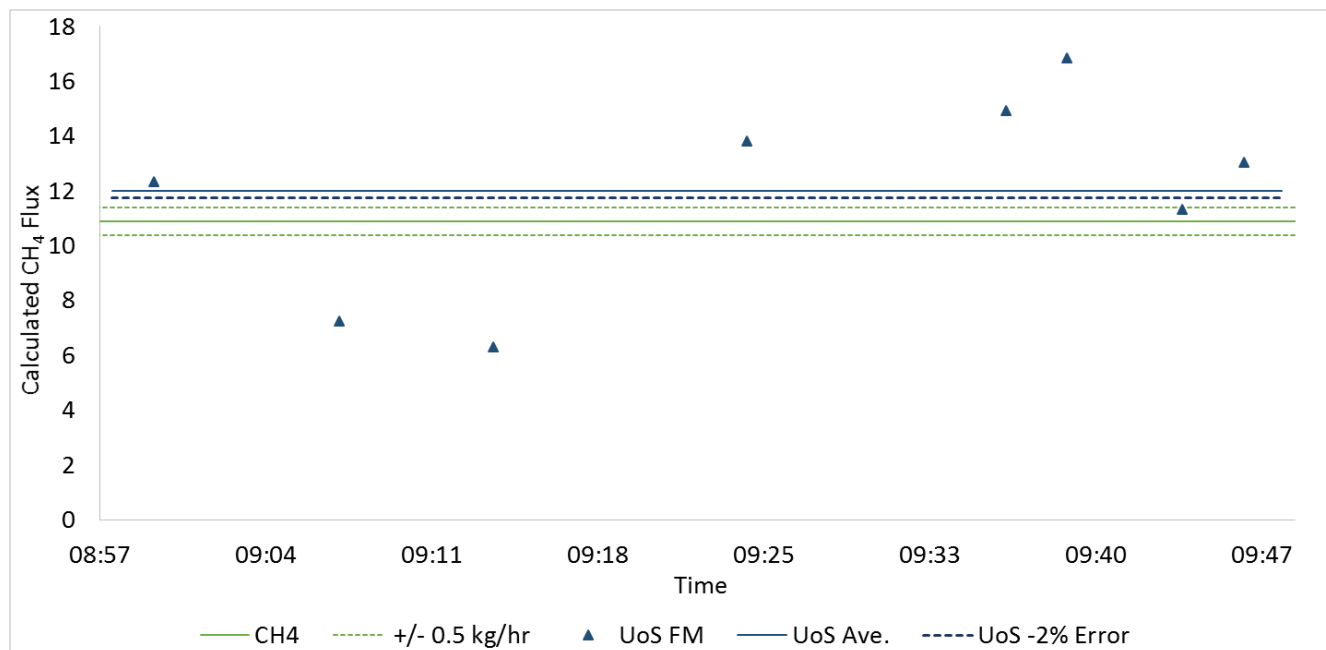
5.4. Discussion of Results

Table E5.6 gives a comparison of the measured CH_4 fluxes with the actual release flux. The measured flux rate is given as the average CH_4 flux including the standard deviation (SD) and assuming a purity of the C_2H_2 of 100%. As discussed in section 3.2.1, the C_2H_2 has a purity of between 98 and100%. A lower concentration will result in a lower CH_4 flux. This is shown in Table E5.6 as a minimum average.

Table E5.6 Comparison between measured and actual CH$_4$ flux rates

Release no.	Actual CH$_4$ flux rate (kg/h)	UoS Measured CH$_4$ flux rate (kg/h)		DTU Measured CH$_4$ flux rate (kg/h)	
		Average ± SD	Minimum average ± SD	Average ± SD	Minimum average ± SD
8	10.9 ±0.5	10.44 ± 0.46	10.23 ± 0.45	9.86 ± 2.22	9.66 ± 2.17
9	10.9 ± 0.5	11.88 ± 3.84	11.64 ± 4.15	10.39 ± 3.30	10.18 ± 3.24
10	10.9 ± 0.5	10.64 ± 1.26	10.43 ± 1.23	11.22 ± 2.72	10.99 ± 2.66
11	5.3 ± 0.2	5.37 ± 0.70	5.26 ± 0.68	4.34 ± 0.25	4.25 ± 0.24
12	10.9 ± 0.5	11.99 ± 3.63	11.75 ± 3.56	-	-

5.4.1. Release 8 Discussion

The UoS made only two transects during Release 8. The data from these transects are very good in terms of low noise and good plume matching. There is an excellent match between the actual and measured fluxes.
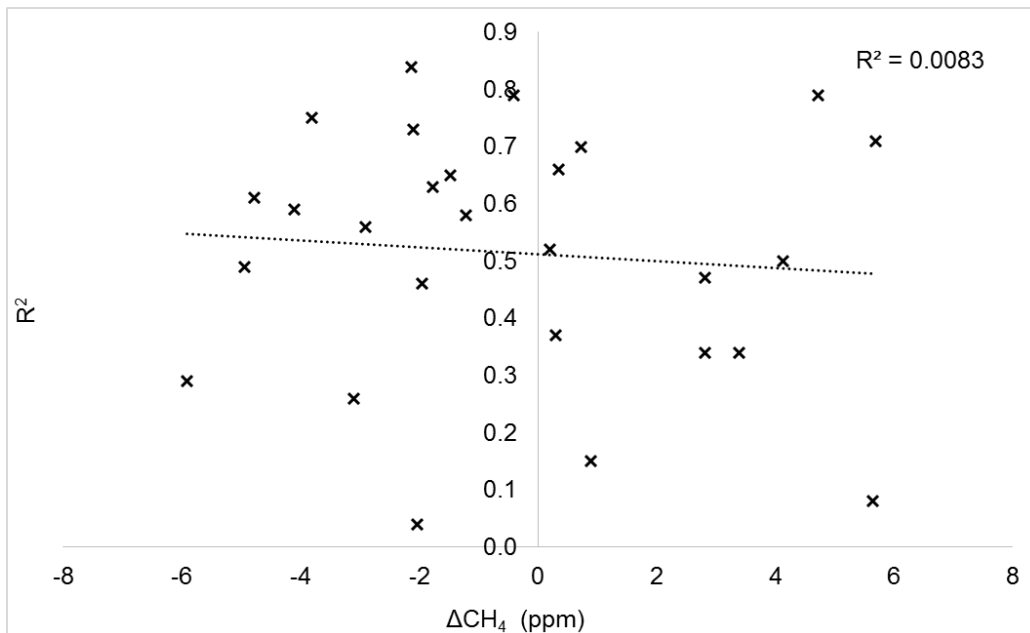
DTU made 20 useful transects during Release 8. Good correlations between CH$_4$ and C$_2$H$_2$ were generally observed. The difference between the measured CH$_4$ flux rate and the actual release flux rate is -8.7% ((measured-actual)/actual and using average values and a C$_2$H$_2$ purity of 100%), and the average measured flux is a little below the range of CH$_4$ release reported by NPL.

5.4.2. Release 9 Discussion

The flux from Release 9 measured by UoS is somewhat higher than the actual release flux: 11.88 kg/h compared to 10.8 kg/h. There is one data point which skews the average, transect UOS 9.10 (Figure E5.4). There is a small off-set between the two plumes in this transect (R^2 0.68). The offset is also apparent in transects UOS 9.9 and UOS 9.11, although it is not as pronounced (R^2 0.76 and 0.73, respectively). In Release 9, the C$_2$H$_2$ and CH$_4$ release points were not co-located but separated by ~140 m (Figure E4.4). During the course of the experiment, the measured wind direction shifted from 235 degrees at the start of monitoring, to 229 degrees during transects UOS 9.9 to UOS 9.11, before coming back to ~236 degrees by the end of the release. The small change in the wind direction relative to the position of the two release points may have resulted in an off-set between plumes, especially if the monitoring distance was not far enough away for full mixing to occur. If transect UOS 9.10 is removed from the analysis, then the average measured flux reduces to 10.8 kg/h although the standard deviation is still high, SD 3.3.

DTU measured 27 useful transects during Release 9. A good correlation between CH$_4$ and the C$_2$H$_2$ plume was obtained. During Release 9, the gas analyser's measurement frequency was reduced. The reason for this is not known. This reduced measurement frequency is likely the cause of lower R^2 compared to measurements performed during Release 8 (see Tables E4.8 and E4.9 in sections 4.2.1 and 4.2.2). The difference between the measured CH$_4$ flux rate and the actual release flux rate is -3.8% and the average measured flux is within the range of CH$_4$ release reported by NPL. The relatively low R^2 values therefore do not signify poor measurement accuracy in this case. A comparison of R^2 with the measured CH$_4$ flux demonstrates that there is no correlation between R^2 and the calculated flux for each transect. Figure E5.8 shows ΔCH$_4$ (the difference between the measured and actual CH$_4$ flux) compared with R^2 for each transect's data. There is no statistical relationship between the data.

Figure E5.8 Comparison between ΔCH_4 and R^2 for DTU Release 9 data

5.4.3. Release 10 Discussion

The UoS measured flux from Release 10 is within <0.2 kg/h of the actual release rate. There is a falling trend in the measured flux, although the reason for this is not clear. There is excellent plume matching for each transect.

A total of 12 useful transects were made by DTU during Release 10. A good correlation between CH_4 and the C_2H_2 plume was obtained. The difference between the measured CH_4 flux rate and the actual release flux rate is +3.9% and the average measured flux is within the range of CH_4 release reported by NPL.

5.4.4. Release 11 Discussion

UoS data show an excellent correlation between the individually measured CH_4 fluxes and the actual release flux.

DTU made six useful transects during Release 11. The difference between the measured CH_4 flux rate and the actual release flux rate is <1 kg/h below the average measured range of CH_4 release reported by NPL. The bigger difference between the measured and the actual CH_4 flux rates could be a result of the fewer transects performed during this release in comparison to the other releases.

5.4.5. Release 12 Discussion

Release 12 saw the highest variability in measured CH_4 flux, with an average of 11.99 kg/h and a standard deviation of 3.63 compared to the actual release rate of 10.9 kg/h ± 0.5. The reason for the high variability is not immediately clear, although the C_2H_2 data contain more noise than in the other releases, especially transects 3 and 6, which were made at a greater distance.

In transects UoS 12.1 to 12.3, the background CH_4 concentrations are the highest measured in all the tests. The reason for this is unclear, but the high background results in a lower measured CH_4 flux. It should be noted too, that the CH_4 and C_2H_2 release locations are not co-located (Figure E4.7). For both these reasons, the R^2 is relatively low on a number of the transects, suggesting poor correlation between the plumes. Further to this, owing to the wind direction during Release 12, there may have been some interference in the CH_4 data from the manure pile, which was exacerbated due to the slow flow-through time of the LGA. This may mean that the simplified analysis method is not valid on all of these transects (see section 5.2 of this appendix).

DTU did not take part in Release 12.

6. Summary and guidance

6.1. Summary of analysis

The release rates (mass flux) of the CH_4 was controlled and regulated by NPL, but not known to the monitoring teams (UoS, DTU and UoM) at the time of the experiment or during the initial analysis of data. Likewise, monitoring data was not shared or discussed between the monitoring teams until after data had been analysed.

For both UoS and DTU there is excellent correlation between the two TDM analyses, the actual CH_4 release and the UoM measured flux rates.

For the UoS data, only Releases 9 and 12 are outside the measurement error of the controlled release rate. In both of these releases, the gas release locations were separated by ~140 m, whereas in all other releases, the gas release points were co-located. In these two tests, many of the plume transects were eliminated due to a significant off-set in the data, reducing the number of data sets. A more comprehensive processing of the data may have improved the comparison. Additionally, where the measured plumes are not directly perpendicular to the wind, where there are bends in the road or the vehicle speed changes, it may be better to correct for the angle off-perpendicular and integrate the plumes with distance rather than time.

A comparison of the UoS and DTU data does not indicate significant differences between the two different monitoring instruments. The lower detection limit of the Picarro analyser (DTU) may, however, be useful when measuring low emission rates or measuring at far distance to the emission source.

The CH_4 flux rates measured in the validation trials are low when compared to what might be expected from a landfill. CH_4 emissions from landfill will vary by landfill size, the waste type and age, site engineering and restoration, and whether there is active gas extraction. Emission rates may be 1 to 2 orders of magnitude greater than those tested here. The measurement, data-processing and analysis techniques would be the same for determining emissions from landfill, however, CH_4 fluxes generated over a larger area may require the release of more C_2H_2 over a spatially wider area. The validation trial has demonstrated the accuracy of the TDM technique at low flux rates. Higher flux rates from localised sources would, in theory, lead to improved accuracy as it would be easier to resolve source-derived CH_4 concentrations against background.

6.2. Operational Guidance

The successful implementation of a tracer gas dispersion test to monitor CH_4 fluxes is dependent on a number of factors. Potential errors can be minimised by paying due regard to the points below.

6.2.1. Constraining methodological errors

Meteorological conditions suitable for the TDM method

The technique relies on any plume arising from the landfill touching the ground at a distance where there has been full mixing of tracer and source gas, but not at distances where dilution of the tracer gas and source means monitored concentrations are just above background (or below the limits of the analyser).

Conditions not conducive to tests include times of high sensible heat fluxes (middle of hot sunny days) and very low wind speeds (<2 m/s).

Changeable meteorological conditions during the course of a release are also undesirable. Changing wind directions may affect the placement of the tracer gas bottles on the landfill.

Assumption of full mixing

The method requires that the dispersion of tracer gas follows the same pattern as the dispersion of the source gas, and very often this is taken to mean that complete mixing of the two plumes is achieved.

Overlapping of tracer and source gas plumes

Tracer and source gas plumes should overlap on a given transect through the plumes. Significantly off-set plumes may indicate that there has not been full mixing of the plumes at the distance measured and this will affect the calculated source flux. In this instance, monitoring further downwind of the source may improve the overlap. Too far downwind, however, and gases may be so dispersed that they are below the detection limits of the analyser above background.

Off-set plumes may also indicate poor placement of the tracer gas bottles in relation to the source and/or wind direction. It may be possible to improve overlap by moving the gas release location on the landfill, especially if the wind direction changes during the course of a release.

Interference from external sources

It is important that external sources are found and isolated through background screening, preferably on days when the wind is constant and from different directions.

6.2.2. Constraining measurement errors

Release of tracer gas

In the experiments described, the tracer gas release rate was calculated by measuring the mass of the C_2H_2 bottle before and after each use. The release rate was controlled manually and was assumed to be constant for the duration. With this method, the precision of the gas bottle weighing, maintaining a constant release rate, and exact timing of the start and end of the release are critical.

If flow meters and/or a low controller are used, they should be properly calibrated and the accuracy and repeatability of the instrument taken into account within the final calculations, along with any corrections necessary for air temperature and pressure.

In either method, the purity of the tracer gas should be accounted for.

Measurement of background

An average background concentration is subtracted from the test data prior to calculating the mass flow. Attaining an accurate and consistent background concentration measurement for each plume transect is, therefore, essential. Sufficient data should be collected on either side of the plume transect to allow an average background concentration to be calculated. Any interfering gases (source gas or tracer) should not be used in the calculation of average background.

6.2.3. Data analysis

Selection and rejection criteria for plume transect data

Data should be rejected where there is significant interference of external sources, or where there is excessive noise in the data.

Where there are significant off-sets between the source and tracer gas plumes, individual transects should be assessed to determine the reason for the off-set. If the off-set is because there had not been full mixing of the gases at the distance measured, then the data should not be used and additional transects should be carried out further downwind of the source. However, if the off-set is due to a change in wind direction relative to the position of the source and tracer release points, then it is possible to use the data to calculate fluxes using Equation E.1.

To improve the accuracy of the final source flux calculation, it is recommended that at least 10 transects are made for each tracer release.

7. Conclusions

Using the TDM technique, accurate and repeatable CH_4 mass flow calculations have been made without prior knowledge of the CH_4 flux rate. Between UoS and DTU, a total of 132 plume transects were made over five CH_4 releases.

The CH_4 fluxes measured by the different teams are comparable and within experimental error.

8. References for Appendix E

BÖRJESSON, G., SAMUELSSON, J., CHANTON, J. (2007) CH_4 oxidation in Swedish landfills quantified with the stable carbon isotope technique in combination with an optical method for emitted CH_4. *Environmental Science & Technology*, 41, 6684–6690.

BÖRJESSON, G., SAMUELSSON, J., CHANTON, J., ADOLFSSON, R., GALLE, B. AND SVENSSON, B.H. (2009) A national landfill CH_4 budget for Sweden based on field measurements, and an evaluation of IPCC models. *Tellus,* B 61, 424–435.

FOSTER-WITTIG T.A., THOMA, E.D., GREEN, R.G., HATER, G.R., SWAN, N.D. AND CHANTON, J.P. (2015). Development of a mobile tracer correlation method for assessment of air emissions from landfills and other area sources. *Atmospheric Environment*, 102 (2015) 323-330.

GALLE, B., SAMUELSSON, J., SVENSSON, B.H. AND BÖRJESSON, G. (2001) Measurements of CH_4 emissions from landfills using a time correlation tracer method based on FTIR absorption spectroscopy. *Environmental Science & Technology*, 35 (1), 21-25.

GOOGLE EARTH v7.1.8.3036. (2017) Cardington Airfield, Lat 52.104, Lon -0.424, elevation ~2 km. 3D Buildings data layer. Infoterra Ltd. & Bluesky 2017. Viewed May 2017 <https://www.google.com/earth/index.html>.

MØNSTER, J.G., SAMUELSSON, J., KJELDSEN, P., RELLA, C. W. AND SCHEUTZ, C. (2014) Quantifying CH_4 emission from fugitive sources by combining tracer release and downwind measurements – a sensitivity analysis based on multiple field surveys. *Waste Management*, 34 (8), 1416-1428.

MØNSTER, J., SAMUELSSON, J., KJELDSEN, P. AND SCHEUTZ C. (2015). Quantification of CH_4 emissions from 15 Danish landfills using the mobile tracer dispersion method. *Waste Management* 35 (2015) 177–186.

ROSCIOLI, J. R., YACOVITCH, T. I., FLOERCHINGER, C., MITCHELL, A. L., TKACIK, D. S., SUBRAMANIAN, R., MARTINEZ, D. M., VAUGHN, T. L., WILLIAMS, L., ZIMMERLE, D., ROBINSON, A. L., HERNDON, S. C., AND MARCHESE, A. J. (2015). Measurements of CH_4 emissions from natural gas gathering facilities and processing plants: measurement methods. *Atmospheric Measurement Techniques*, 8, 2017-2035.

SCHEUTZ, C., SAMUELSSON, J., FREDENSLUND, A. M. AND KJELDSEN, P. (2011). Quantification of multiple CH_4 emission sources at landfills using a double tracer technique. *Waste Management*, 31 (5), 1009-1017.

Would you like to find out more about us or about your environment?

Then call us on
03708 506 506 (Monday to Friday, 8am to 6pm)

email
enquiries@environment-agency.gov.uk

or visit our website
www.gov.uk/environment-agency

incident hotline 0800 807060 (24 hours)
floodline 0345 988 1188 / 0845 988 1188 (24 hours)

Find out about call charges: www.gov.uk/call-charges